

FACILITY FORM 602

N66 37569

(ACCESSION NUMBER)

88

(PAGES)

CI-78361

(NASA CR OR TMX OR AD NUMBER)

(THRU)

1

(CODE)

31

(CATEGORY)

SID 66-1277

QUARTERLY REPORT NO. 1
(May-July 1966)
A STUDY OF ELECTRONIC PACKAGES
ENVIRONMENTAL CONTROL SYSTEMS
AND VEHICLE THERMAL SYSTEMS
INTEGRATION
(Contract NAS 8-20320)



29 July 1966

GPO PRICE \$ _____

CFSTI PRICE(S) \$ _____

Hard copy (HC) 3.00

Microfiche (MF) .75

7 653 July 65

D. J. Watanabe

D. J. Watanabe
Project Manager

Approved by:

G. A. Stevenson
G. A. Stevenson, Chief
Environmental Control
and Life Support Systems

Approved by:

W. H. T. Loh
W. H. T. Loh, Director
Aerothermal and Power Systems
Department

NORTH AMERICAN AVIATION, INC.
SPACE and INFORMATION SYSTEMS DIVISION

[Handwritten signature/initials]

SID 66-1277

QUARTERLY REPORT NO. 1
(May-July 1966)
A STUDY OF ELECTRONIC PACKAGES
ENVIRONMENTAL CONTROL SYSTEMS
AND VEHICLE THERMAL SYSTEMS
INTEGRATION
(Contract NAS 8-20320)



29 July 1966

D. J. Watanabe

D. J. Watanabe
Project Manager

Approved by:

G. A. Stevenson

G. A. Stevenson, Chief
Environmental Control
and Life Support Systems

Approved by:

W. H. T. Loh

W. H. T. Loh, Director
Aerothermal and Power Systems
Department

NORTH AMERICAN AVIATION, INC.
SPACE and INFORMATION SYSTEMS DIVISION



FOREWORD

This document is submitted by the Space and Information Systems Division (S&ID) of North American Aviation, Inc. to the George C. Marshall Space Flight Center (MSFC) of the National Aeronautics and Space Administration in accordance with Contract NAS 8-20320 . This report summarizes the study activity conducted during the first quarter of the contract.

TECHNICAL REPORT INDEX/ABSTRACT

ACCESSION NUMBER				DOCUMENT SECURITY CLASSIFICATION			
				Unclassified			
TITLE OF DOCUMENT						LIBRARY USE ONLY	
QUARTERLY REPORT NO. 1, A STUDY OF ELECTRONIC PACKAGES ENVIRONMENTAL CONTROL SYSTEMS AND VEHICLE THERMAL SYSTEMS INTEGRATION							
AUTHOR(S)							
Watanabe, D. J.							
CODE	ORIGINATING AGENCY AND OTHER SOURCES			DOCUMENT NUMBER			
NAJ65231	Space and Information Systems Div. of NAA, Downey, California			SID 66-1277			
PUBLICATION DATE			CONTRACT NUMBER				
29 July 1966			NAS 8-20320				
DESCRIPTIVE TERMS							
<p>Environmental Control</p> <p>Thermal Control</p> <p>Thermal Analysis</p>							

ABSTRACT
<p>Study to determine the optimum environmental control (passive or active) systems for thermally conditioning individual electronic packages for space missions of durations ranging from 4½ hours to 180 days. The environmental control system shall be optimized on the bases of mission duration, operational temperature limits and heat dissipation rate of the electronic package.</p> <p>This quarterly progress report describes the work accomplished in establishing the basic requirements and constraints, the survey effort in determining the developmental trends, and the parametric study of thermal control processes and components.</p>



CONTENTS

Section		Page
1.0	INTRODUCTION AND SUMMARY	1
2.0	CURRENT STUDY STATUS	4
	2.1 System Requirements and Constraints	4
	2.2 Component and Subsystem Review and Evaluation	31
	2.3 Parametric Study and Trade-Off Analysis	54
3.0	FORECAST FOR NEXT QUARTER	81



ILLUSTRATIONS

Figure		Page
1.	Program Schedule	3
2.	Power Source Spectrum	10
3.	Vehicle Orbit and Orientation	13
4.	Absorbed Heat - Earth Polar Orbit	14
5.	Absorbed Heat - Synchronous Equatorial Orbit	15
6.	Absorbed Heat - Lunar Polar Subsolar Orbit	16
7.	Evolution of Parts - Electronic Systems	19
8.	Reduction Obtained with Integrated Circuits	19
9.	Microelectronic Techniques	20
10.	Microelectronics	22
11.	Large Scale Multifunctional Arrays	23
12.	Cross Sections of Conventional and Thermoelectric Coldplates	33
13.	Coolant Supply Temperature Versus Thermoelectric Input Power/Package Heat Load	34
14.	Pin-fin Coldplate Configurations	37
15.	Pin-fin Coldplate Performance	38
16.	Pin-fin Coldplate Flow Pattern	40
17.	Compounds for Low Temperature Operation	52
18.	Manifold Weight Versus Mission Time	55
19.	Manifolding Concepts	57
20.	Manifold Weight Versus Mission Time	58
21.	Space Radiator Performance	60
22.	Radiator Surface Temperature Versus Coolant Outlet Temperature	63
23.	Coolant Inlet Temperature Versus Equipment Heat Load	65
24.	Radiator Temperature Versus Absorbed Incident Radiation	66
25.	Q_{min}/Q_{max} Ratio Versus Sink Temperature	69
26.	Viscosity Multiplication Factor Versus Flow Rate	71
27.	Viscosity Versus Radiator Outlet Temperature	72
28.	Viscosity Versus Equipment Heat Load	74
29.	Radiator Efficiency Versus Ratio	75
30.	Equilibrium Temperature Versus Ratio	77



TABLES

Table		Page
1.	System Requirements and Constraints	5
2.	Possible Future Space Missions	7
3.	Possible Future Space Missions	8
4.	Orbital Elements and Planetary Data	12
5.	Computer Characteristics Summary	28
6.	GP Computer Requirements	29
7.	Comparison of S-16 OSO Thermal Control Test Surfaces	42
8.	Comparison of S-17 OSO Thermal Control Test Surfaces	44
9.	Test Surfaces Selected for S-57 OSO	45
10.	Possible Organic Coolants	51



1.0 INTRODUCTION AND SUMMARY

This study is directed toward defining environmental control system (ECS) concepts to meet the increased complexity and changing thermal conditioning requirements of the electronic equipment on the Saturn V vehicle for missions of durations varying from four and one-half hours to one-hundred eighty days. The study objective is to establish the optimum environmental control concepts for thermally conditioning individual electronic packages. Essential characteristics of the optimum environmental control systems are maximum practicable reliability, maximum operating range, minimum weight, minimum power, and minimum volume. The optimum systems are to be selected on the basis of future Saturn mission requirements, future trend in the design and development of the electronic equipment and being an integral part of the overall vehicle thermal system.

The results of the study effort will help to define the developments and advancements required in the technology of thermal control methods and systems. Critical areas or pacing items for development are to be identified. This should help to insure the necessary development to be accomplished and on a timely basis. Other results from the study include design guidelines for electronic packages to achieve optimum environmental control designs and for integrated ECS and vehicle thermal control systems.

Longer mission duration and greater heat dissipation requirements together with closer temperature regulation require thermal systems in which the control method is self regulating and is capable of operating under widely varying conditions. The simple passive system cannot meet these requirements. The study effort is directed toward the investigation of system concepts which can function reliably within widely varying conditions. These systems concepts, like the simple passive system, will depend upon rejecting waste heat to space, but the means of transporting heat from the source to the radiating surface and the surface itself will be quite different. The systems will be more complex than the pure passive approach and thus it becomes a challenge to achieve practical, simple and reliable systems. Many alternate concepts are to be investigated and the most promising ones are to be studied in depth.



SUMMARY

The study effort has progressed in accordance with the study plan in meeting the schedules and in performing the planned tasks. The schedule position and the major tasks performed during this reporting period are indicated in Figure 1.

The basic requirements and constraints to be used as the guidelines for the study of the thermal control systems have been established except for defining the specific thermal requirements of the astrionic equipment. In establishing the requirements and constraints, typical or representative future Saturn mission and vehicle combination which include earth orbital and lunar missions have been selected. For these missions, a relatively simple environmental model has been assumed. The most significant environmental factor is the incident heat loads, which have been established for the various surface orientation of a simulated cylindrical structure. This data is to be used to establish the maximum and minimum heat load conditions which will depend upon the vehicle attitude in flight, the surface orientation with respect to the heat sources, vehicle spin rate and the spin axis.

The survey of current and new developments in astrionic equipment and thermal control components and processes has been initiated and is being continued. The trend toward microminiaturization of astrionic equipment is definitely indicated with the associated lower heat loads and closer temperature regulation. The heat load profiles, temperature ranges and temperature regulation associated with the various representative Saturn mission are to be established. In the area of thermal control components or processes, the survey effort up to this point indicate no significant new developments. Further survey effort is continuing to determine if there are any new developments in this area. One of the expected results from this study effort is to indicate what new developments are required for future thermal control systems associated with astrionic equipment applicable to future Saturn vehicle.

Parametric study was initiated in several areas which are basic to a thermal control system. These areas include manifolding, space radiator design, coolant viscosity and α/ϵ ratio selection. The parametric effort is directed toward providing data in easy to use form which can be readily used for either performance evaluation or comparative evaluation in the selection of components or processes.

Based on the results of the study effort during this reporting period, no change in the study plan appear necessary. The schedule and the tasks to be performed are considered to be satisfactory to meet the ultimate objectives of the contract work.



April 20, 1966

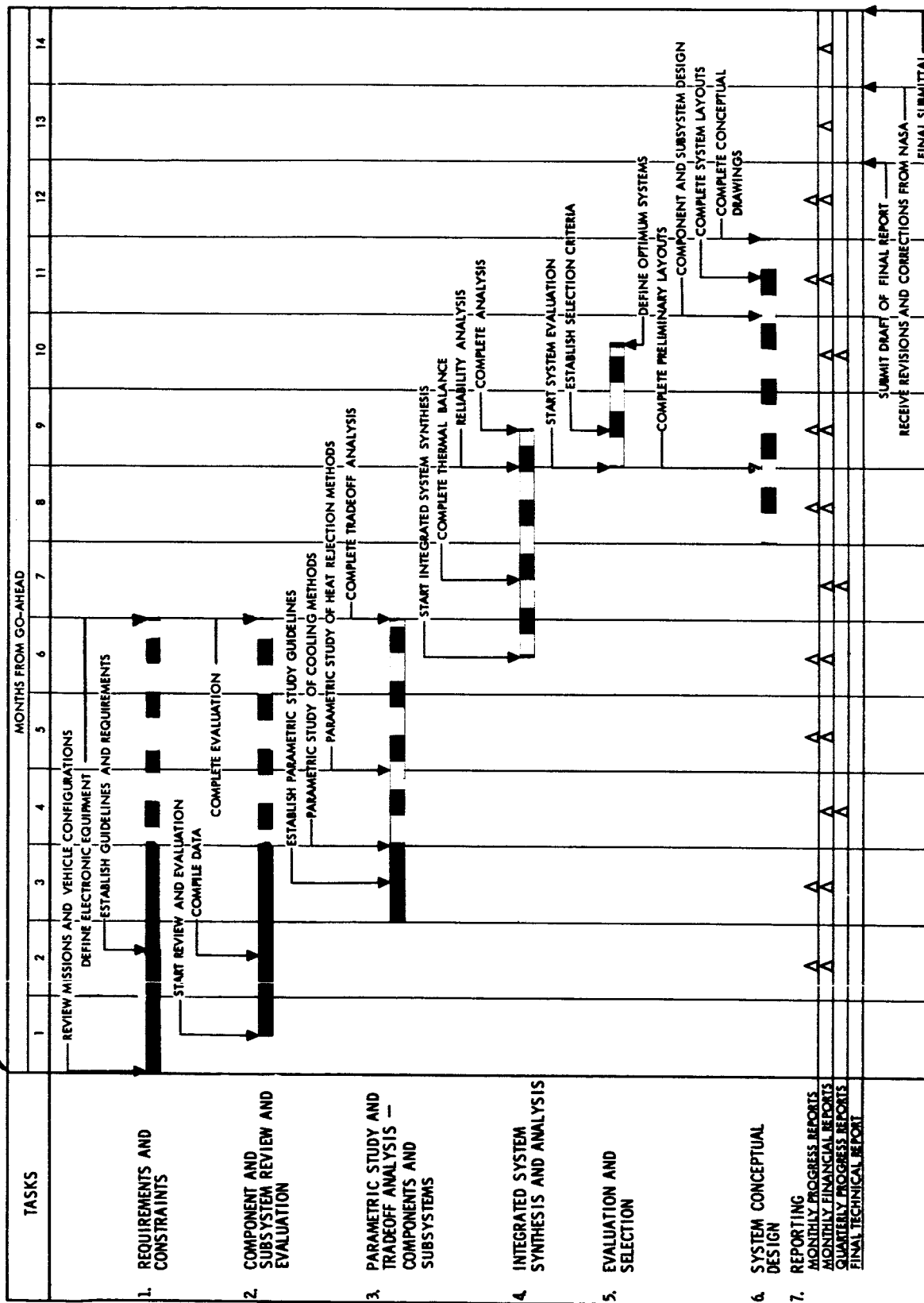


Figure 1. Program Schedule



2.0 CURRENT STUDY STATUS

2.1 SYSTEM REQUIREMENTS AND CONSTRAINTS

System requirements and constraints have been established to provide the basic guidelines for the study effort. The requirements and constraints encompass the range of values or conditions that are representative for the foreseeable future missions. It is based on a survey of future missions under consideration by NASA and others. For the purposes of this study, future missions have been categorized as: near earth orbital mission, synchronous earth orbital mission, and lunar mission. These missions are considered adequate to define the thermal requirements and mission/vehicle constraints which may be expected for the future missions with $4\frac{1}{2}$ hours to 180 day mission duration. The near earth orbital mission is considered to include missions such as orbiting research laboratory (AORL, MORL, LORL) and the staging phase of planetary or lunar missions. The synchronous orbital mission is considered to include communications, and command and control type missions. The lunar mission includes the lunar orbiting and landing and lunar ferry missions, and both can be, considered to be either direct earth launch or orbital launch.

Table 1 summarizes the requirements and constraints that will be used for the study effort. As indicated in Table 1, the vehicle configuration has been assumed to be basically the Saturn V, with various combinations of the instrument unit or units with the up-rated upper stages or spacecraft. This provides the general design constraints as to the size or volume of the thermal control systems. Also indicated in Table 1, circular orbits have been selected in order to simplify the calculations for incident heat loads. It is assumed that these calculated values are sufficiently representative even for elliptic type orbits.

One of the necessary requirements for the thermal system is that it shall be fully automatic and capable of being controlled from the ground or from an orbiting spacecraft. It is assumed for certain missions, the thermal system may be on a long term stand-by in orbit and later activated as required. Another system requirement is no maintenance provisions or requirements, since it is assumed the crew will not be available to perform the task and also since the thermal system may not be accessible for maintenance.

Those items in Table 1 which are to be established are discussed in the following paragraphs. These items are more closely associated with the specific missions and thus are established for each mission.



Table 1. System Requirements and Constraints

Mission/Vehicle Data	Requirements and Constraints
Astrionic Equipment: (to be established)	Heat Load (to be established) Temperature Regulation (to be established) Temperature Range (to be established)
Orbit or Trajectory: a) 200 nautical mile circular earth orbit b) Synchronous earth equatorial orbit c) 80 nautical mile circular lunar orbit	Space Environment: Zero gravity Low density Thermal radiation (to be established)
Vehicle Configuration: Saturn V	IU integral with up-rated upper Saturn stages, or with spacecraft in some cases.
Mission duration	4½ hours to 180 days
Operational time period	1968 and beyond
Maintenance	No provisions
Control Method	Automatic
Reliability Goal	(to be established)
Interface Requirements	None



2.1.1 Future Space Missions

A survey of information on future space missions was made to obtain mission data required to establish the basic guidelines. It was limited to current studies and technical articles on future missions which utilizes the Saturn stages, both current and modified or up-rated design. The missions of interest were those that fell within the range of $4\frac{1}{2}$ hours to 180 day duration.

A list of possible future missions is given in Tables 2 and 3, which include some basic mission data. The information given in these tables plus other data available were used to establish the basic missions, which have been categorized as: near earth orbital mission, synchronous earth orbital mission, and lunar mission. The specific mission designations in current use which fall within the three general categories are indicated in Table 3. The system requirements and constraints established on the basis of the three selected missions are considered to cover the spectrum of future requirements and constraints for thermal systems. This provides a realistic basis for the synthesis, evaluation and selection of integrated electronic packages environmental control and vehicle thermal systems.

For the missions selected, several assumptions were made with regards to the mission characteristics. One assumption is that the orbits are circular and at altitudes that minimizes the radiation and other environmental hazards. Also, it is assumed that the operational time period would be selected to help minimize the environmental hazards. These assumptions permit the use of a relatively simple environmental model. Another assumption is that no crew will be available to perform any maintenance or repairs or be required in the operation of the thermal system. This means the system must be fully automatic and self-contained. However, it should be capable of being controlled from some remote point such as a ground station or an orbiting spacecraft.

2.1.2 Power Supply Considerations

For those thermal control methods or systems which require electrical energy, the power system must be taken into consideration to properly evaluate and to compare the various systems. For the purposes of this study, a few basic data of power systems are all that is considered necessary.

The most important is the power system weight and the apportionment of the weight. To establish the apportionment chargeable to the thermal system, a power weight penalty expressed as



Table 2. Possible Future Space Missions

Missions	Unmanned	Manned Developmental	Manned Operational
Earth Orbital	1958 Unmanned Satellites Scientific Satellites Small special purposes Orbiting observatories Application Satellites Communication Meteorology Navigation Engineering research	1962-68 Manned Satellites Mercury Gemini Apollo Maneuvering reentry Interim orbital labs	After 1968 Orbital Operations Manned orbiting labs Operational ferry vehicle Recoverable boosters Engineering experiment and development
Lunar	1962-68 Lunar Probes Ranger Surveyor Intermediate Space Probes	Before 1970 Manned Landing Apollo Lunar Logistic Systems (Unmanned)	After 1970 Lunar Station Scientific Observations Lunar Explorations
Planetary	1962 Deep Space Probes Mariner Voyager Reference: Astronautics & Aeronautics, Vol 2 No. 12 Dec. 64. p. 23	After 1975 Manned Expeditions Mars Landing Venus Reconnaissance	After 1980 Planetary Operations Mars Station Advanced Manned Expeditions Jupiter Satellites Mercury Others



Table 3. Possible Future Space Missions

Mission	Designation	Mission Data		Mission Vehicles			Launch Methods			
		Duration	Operational Time Period	Spacecraft	Booster or Propulsion	Support	Direct	Orbital	In-Transit Rendezvous	Target Planet Orbital Rendezvous
Earth Orbital	AES (AAP)	30-45 days	1968	Apollo/CM	S-V	-	x	-	-	-
	MORL	1 year	1972	Modified S-IVB	S-V	Spent Stage Utilization	x	-	-	-
	LORL	1-5 years	1977		S-V	Spent Stage Utilization	x	-	-	-
Lunar	Apollo	14 days	1969	Apollo/LEM	S-V	-	x	-	-	-
	Lunar Ferry		1980-85	Command Module and Pallets	Nuclear Propulsion	-	-	x	-	-
	Lunar Base (Temporary)		1974	S-IVB Utilization	S-IVB	-	-	x	-	-
Planetary	Voyager			Apollo/CM (Unmanned)	S-V	-	x	-	-	-
	Mars/Venus Flyby		1975	New Design	S-IVB	LOX Tanker	-	x	-	-
	Mars Landing		1983-88	Apollo/CM Apollo/CM New Design	S-IVC New Multi-Stage Design		-	x	-	-



pounds per kilowatt will be used. This is reasonably accurate and suitable for this study effort. A range of values between 200 to 500 pounds per kilowatt for the power weight penalty has been selected on the basis of available estimates of power system weights as given in Figure 2. This range of values is representative of the expected power penalties for the power systems that may be available for the time period of interest. No attempt is made to define the power system, but only to give the expected trend in the systems weight for the longer duration missions.

In the assessment of the reliability of the thermal systems which depend upon the power system, the possibility of degraded or reduced power supply and emergency power situations are to be considered. For these possible situations, the degraded or alternate operational modes for the thermal system will be investigated.

The possibilities of thermal integration, the sharing of common components and the utilization of by-products such as water from fuel cells may be considered, but until the power systems are better defined, these possibilities will be considered to be of secondary importance.

2.1.3 Space Environment

For the purposes of the study, a relatively simple model for the space environment is considered adequate. The significant environmental factors are: low density or vacuum condition, zero gravity, and thermal radiation. The other environmental factors are considered to have negligible effects. This is based on the assumption that mission trajectories and operational time periods will be selected to minimize environmental hazards. However, it is recognized that the thermal coatings on the space radiator could be affected by the space environment. Over an extended period of time, meteoroids could have an erosive effect on radiating surfaces so that the spectral properties would be altered and the radiating quality of the surface would be reduced. Also, meteoroid impacts could result in puncture of space radiator tubes. Currently, there are insufficient data to define accurately the meteoroidic environment for purposes of evaluating risk and damage. Thus, for this study, the effects of the degradation of the thermal coatings will be assessed, but the probability of puncture of the radiator tubes will be considered negligible.

Thermal radiation from planetary bodies striking on the vehicle surface is a prime consideration in designing a thermal control system. For this reason, incident heat loads have been obtained

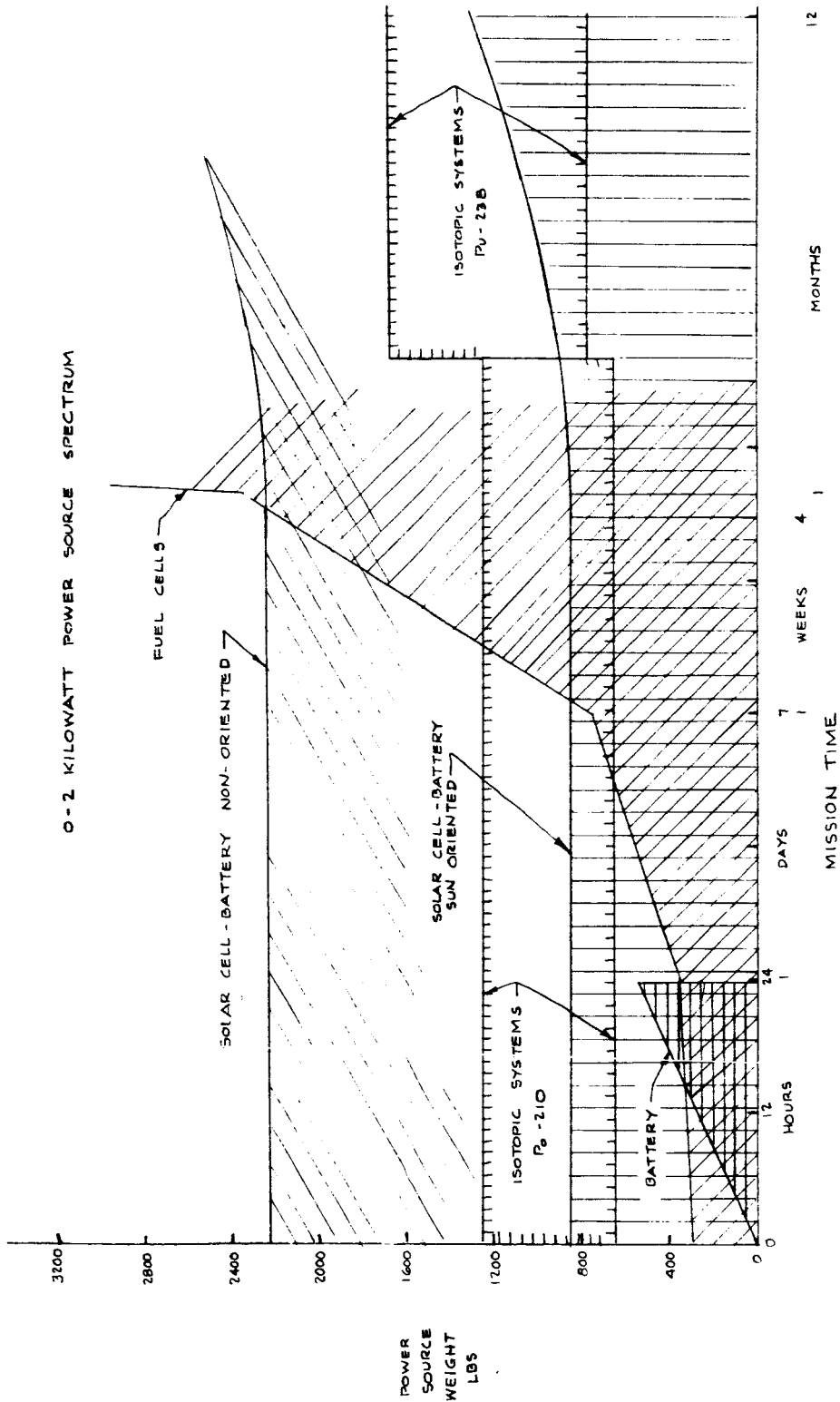


Figure 2. Power Source Spectrum



for a simulated spacecraft in both earth and lunar orbit. These incident heating rates were obtained with the aid of an IBM 7094 digital computer program, which calculates direct solar radiation, planet reflected solar radiation, and planet emitted radiation for each vehicle surface as a function of orbital position. The computer program is one of several developed at NAA and is described in ASD Technical Note 61-83.

The computer program was used to calculate incident heat loads for a polar earth orbit at a vehicle altitude of 200 nautical miles, a synchronous earth equatorial orbit, and a lunar polar orbit at a vehicle altitude of 80 nautical miles. All three orbits were calculated for the eightieth day, and hence, include the subsolar point. Table 4 lists the pertinent orbital elements and planetary data for all three cases. The relative positions of the equatorial plane, the orbit plane, and the spacecraft are shown in Figure 3.

To avoid needlessly complicated expressions for obtaining shadow intersection points, three simplifying assumptions concerning shadow geometry are made in the computer program. These are:

1. The earth is assumed spherical with its radius equal to 3960 statute miles.
2. The earth's shadow is assumed cylindrical and umbral (sun at infinity).
3. Atmospheric refraction and penumbral effects are neglected.

The validity of these assumptions was verified through telescopic observations of satellites as they entered the earth's shadow. Actual entrance times observed during several transits of 1959 Alpha II and 1960 Iota I usually differed from predictions by only a few seconds.

Typical computer results are shown in Figures 4, 5, and 6 for one of the ten vehicle surfaces (surface 1 in Figure 3) in each of the three orbits under consideration. The x-axis was taken to be along the orbit path (in the direction of vector \vec{R}_1) in all three cases, and the value of the solar constant was fixed at 443 Btu/hr-ft². The earth's albedo was based on a value of 0.35, while radiation of the lunar surface was calculated on the basis of a black body at a temperature of 242°F. This last assumption results in a lunar emission of 415 Btu/hr-ft² and a planetary albedo of 0.054. It should be noted that, rather than incident heat loads, Figures 4, 5, 6 show absorbed heat which is dependent on the solar absorptivity, α , and the infrared emissivity, ϵ , of the specific thermal coating used. The set of values ($\alpha_s = 0.2$ and $\epsilon = 0.9$) was selected as being representative of the possible coatings for the ECS radiators.



Table 4. Orbital Elements and Planetary Data

	Polar Earth Orbit	Synchronous Earth Orbit	Polar Lunar Orbit
Epoch of orbital elements	80	80	80
Semi-major axis	4,190 stat. miles	26,180 stat. miles	1172 stat. miles
Eccentricity	0	0	0
Right ascension of ascending node	0	0	0
Argument of perigee	0	0	0
Inclination	90 deg.	0	90 deg.
Orbit period	1553 hours	23.9 hours	2.04 hours
Solar constant	443 Btu/(hr)(sq ft)	443 Btu/(hr)(sq ft)	443 Btu/(hr)(sq ft)
Albedo	0.35	0.35	0.054

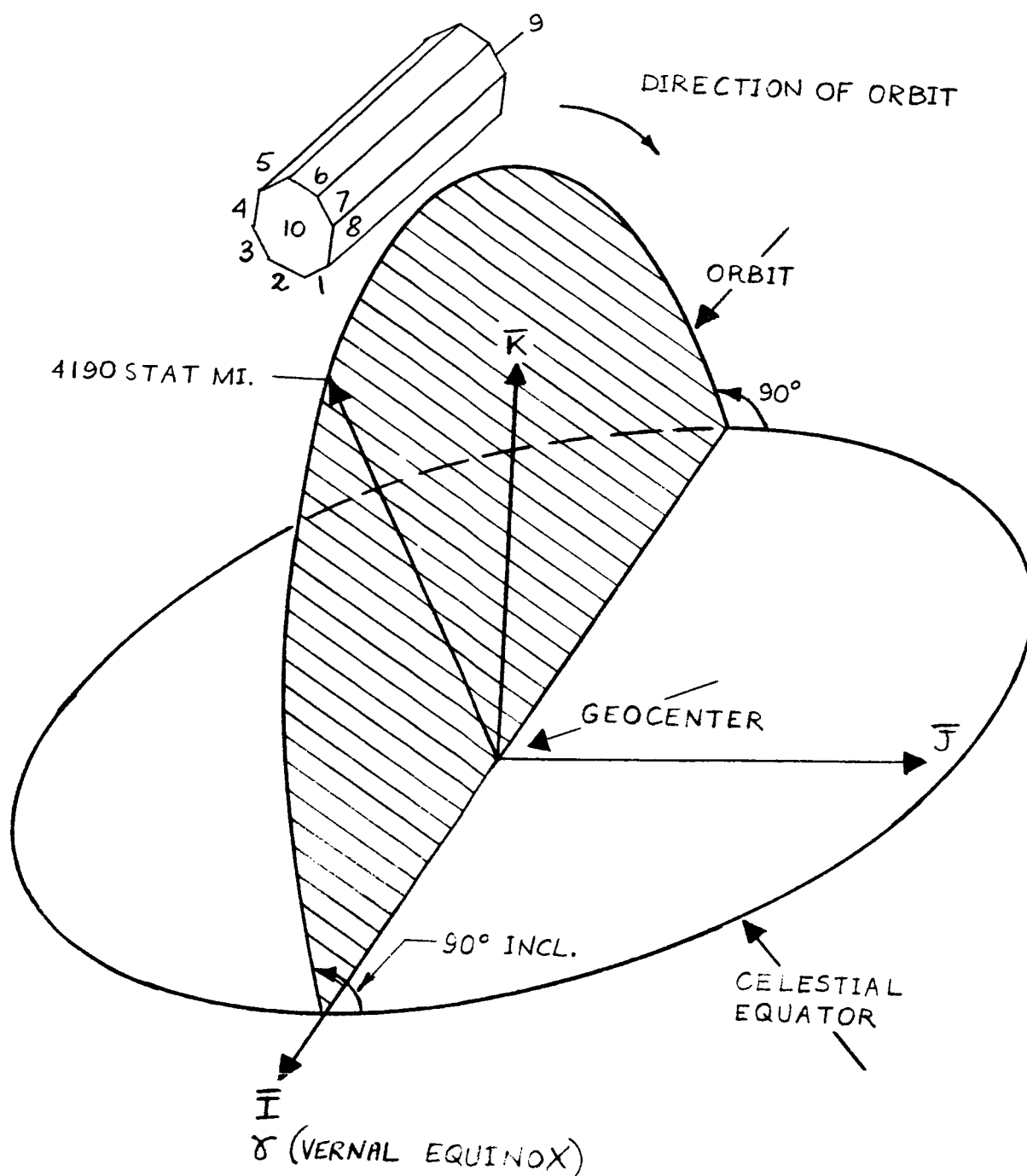


Figure 3. Vehicle Orbit and Orientation

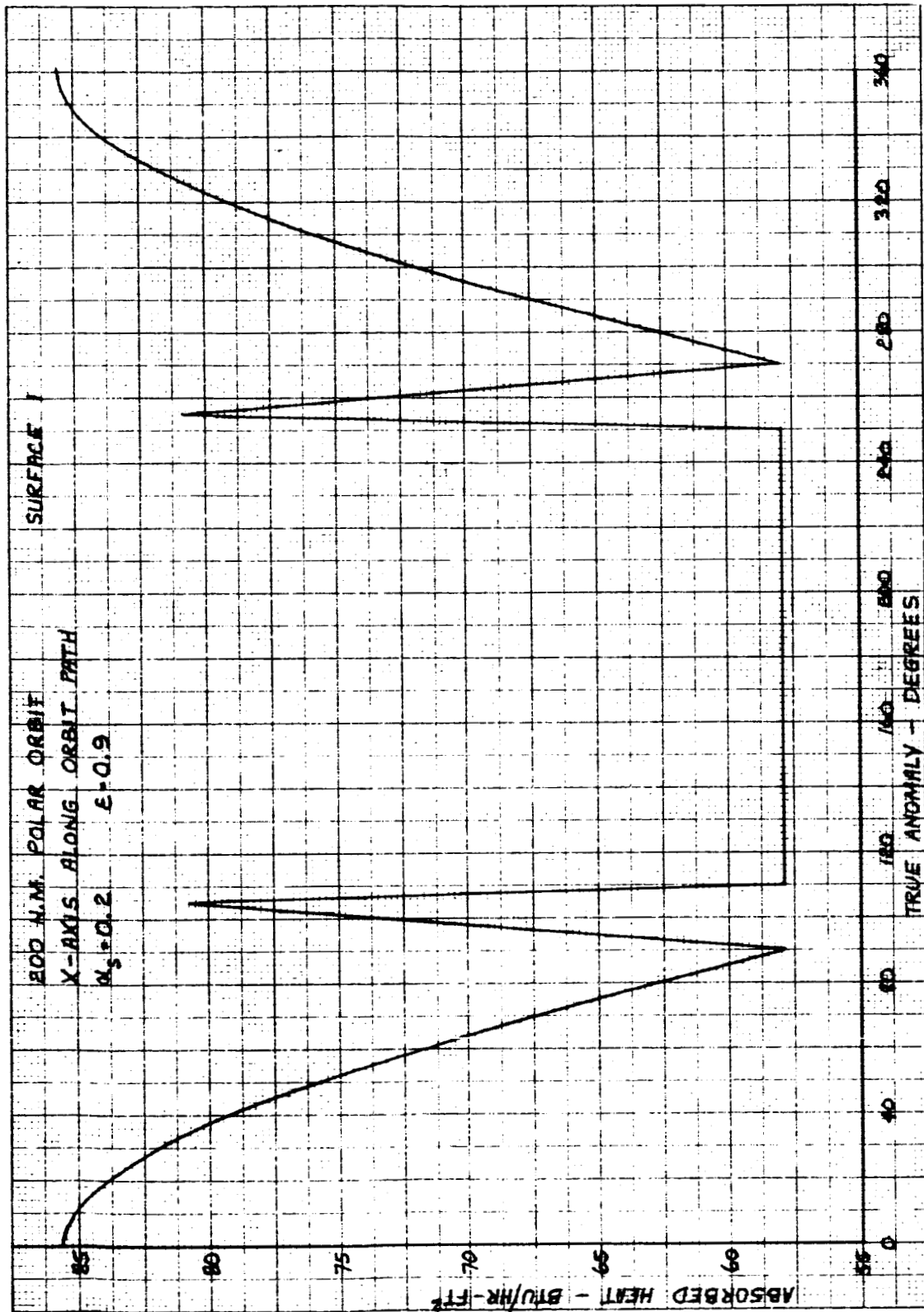


Figure 4. Absorbed Heat - Earth Polar Orbit

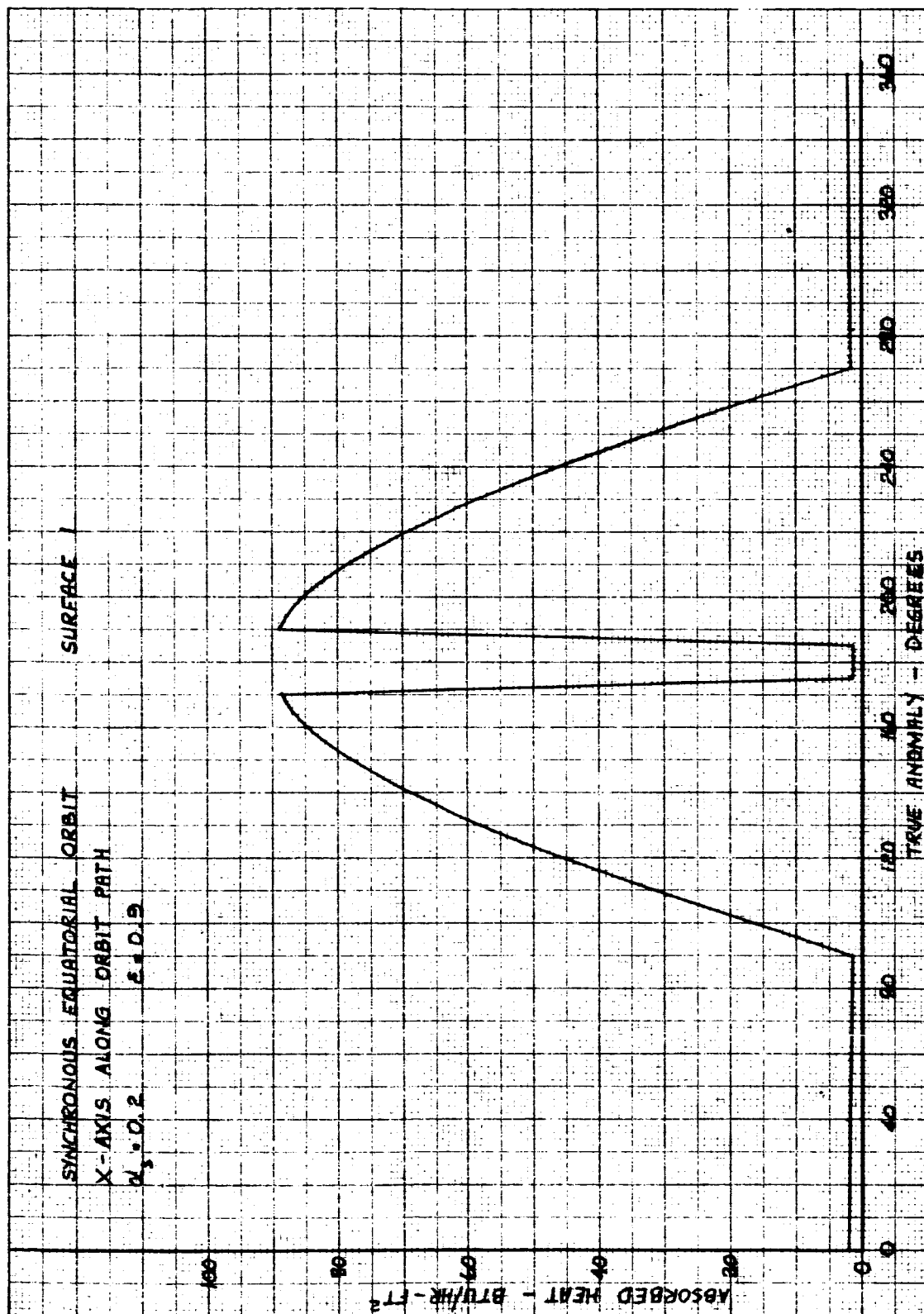


Figure 5. Absorbed Heat - Synchronous Equatorial Orbit

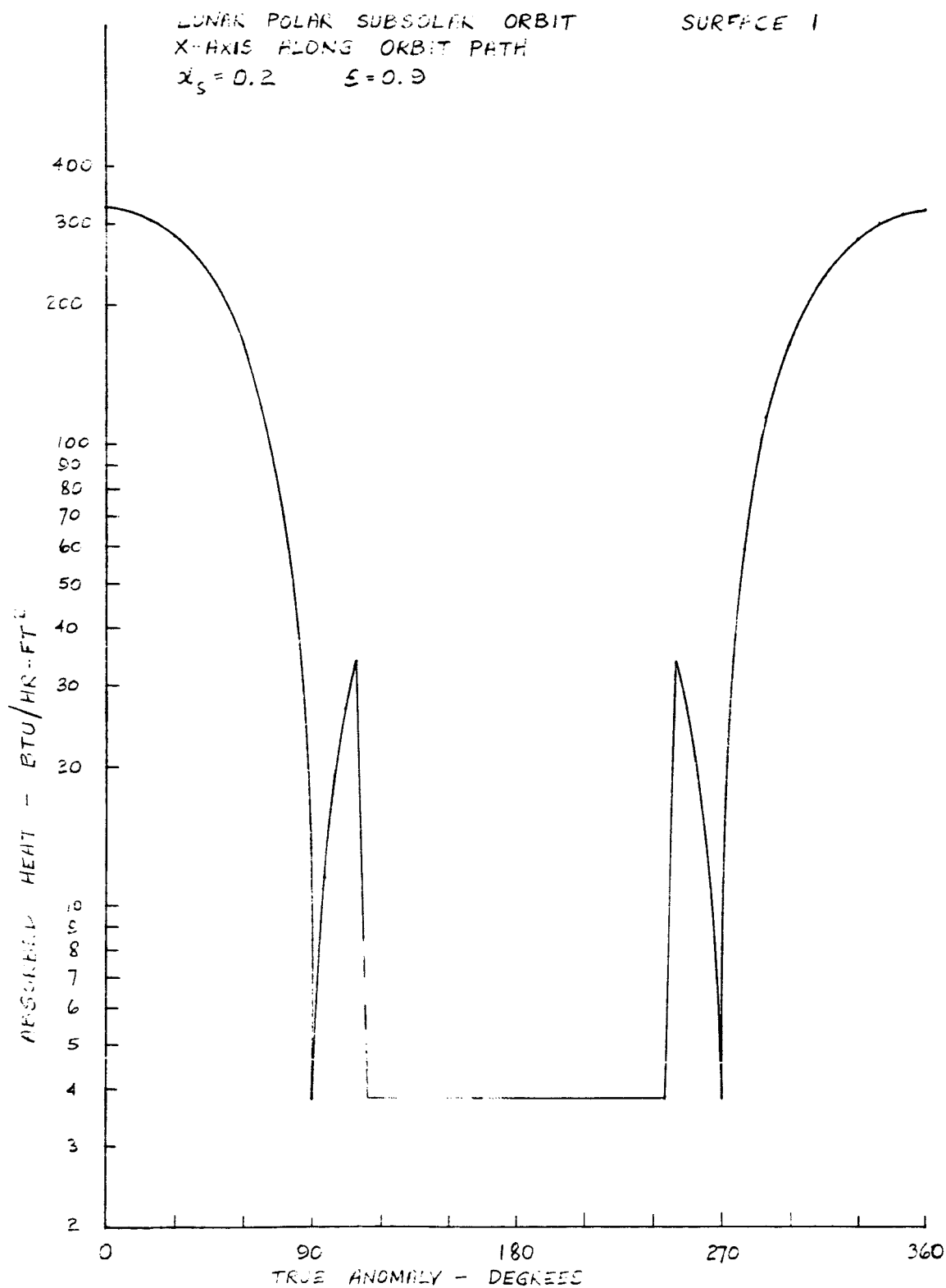


Figure 6. Absorbed Heat - Lunar Polar Subsolar Orbit



Other combinations of α_s and ϵ will result in different values of absorbed heat than those shown in Figure 4, 5, 6, which are intended only to indicate the type of information available from the computer program. Additional assumptions which apply to the curves presented are that the absorptivity to reflected solar radiation equals the solar absorptivity of the coating used, and that the infrared absorptivity equals the infrared emissivity.

Curves such as those in Figures 4, 5, and 6 will be used to establish required space radiator areas and preferred locations on the vehicle. With the selected vehicle orientation, for example, surface 1 always faces the earth or moon, respectively. As a result, it is subject to a constant amount of earth emitted radiation when the spacecraft is in a low altitude earth orbit. This situation is indicated in Figure 4, which shows a relatively high level of absorbed heat (58 Btu/hr - ft²) even when the spacecraft is completely within the earth's shadow. In lunar orbit and when facing the illuminated side of the moon, the surface 1 location is not suitable for a space radiator because the rate of heat absorption due to lunar emission is excessive, as is evident from an examination of Figure 6.

2.1.4 Astrionic Equipment Requirement

To properly set the stage for the requirements, and constraints imposed on and by the astrionics, this section of the quarterly report will discuss the revolution taking place in the electronics industry. The primary instrument considerations with regard to thermal conditioning and thermal integration with the vehicle are the individual and total package heat loads and the degree of package internal temperature regulation required. The first consideration is intimately involved in the state-of-art of micro-miniaturization. The second is related to the inherent maximum and minimum temperature limits of circuit or equipment components. These limits are essentially a matter of reliability, which again are influenced strongly by microelectronics.

Microminiaturization - Trends and Effects

Electronics is presently involved in a microminiaturization revolution, or perhaps more properly, an evolution. The functional complexity of space vehicles demands smaller, lighter-weight, more reliable and lower power system implementation. Microelectronics is unrivalled in all respects for this task.



Microminiaturization, as the name implies, was initially an attempt to reduce size. It is generally recognized today that the fall-outs from this size reduction reap far greater benefits and have more significant impact than the initial goal. (Therefore, the term "microelectronics" is more appropriate.) Paramount among the fall-outs is increased reliability. Almost as important for space applications is the low power requirement, which in turn proportionately reduces the weight and size of both the power supply (such as a battery) and the vehicle ECS. These reduced weight and size, along with the reduced size and weight of the astrionic equipment themselves, increases payloads, permits more complex missions, and/or allows even higher reliability such as through redundancy techniques or through "built-in test" capability for pre-launch and manned in-flight maintainability.

Despite rapid changes taking place, microelectronics is perhaps more evolutionary rather than revolutionary. This is illustrated by Figure 7. The first miniaturization was "miniature" vacuum tubes in the early 1940's, then the "sub-miniature" tubes. The large jump in the miniaturization process was the discovery of the semiconductor devices, the germanium and silicon diodes, soon followed by the transistor in the late 1940's. The transistor today replaces all but the highest power or special purpose vacuum tubes. It is much smaller than the smallest tube and they required no heater (filament) power. The use of transistors was significantly advanced with the development of the "printed" or "etched" circuit techniques. "First generation" microelectronics reached its ultimate form when integrated circuits (IC's) replaced groups of transistors, resistors, capacitors, diodes, etc. The year 1962 represents perhaps the birth of microelectronics when an entire production weapon system, the Minuteman II, went completely to microelectronics. Its D-37 computer used integrated circuits exclusively and is largely responsible for "arrival" of the IC's. The improvements obtained with IC's are illustrated in Figure 8.

Figure 9 shows examples of the four important microelectronic approaches that have been advanced in recent years. The 3D packaging technique is one of a number of compact packaging approaches. These techniques were based on miniature versions of more or less conventional discrete circuits elements - often with a disciplined geometry in order to facilitate the compact packaging. With such an approach, each component provides only one circuit element and so the number of parts is not reduced, the economics of the system is not significantly affected, and heat reduction is also not significantly affected.

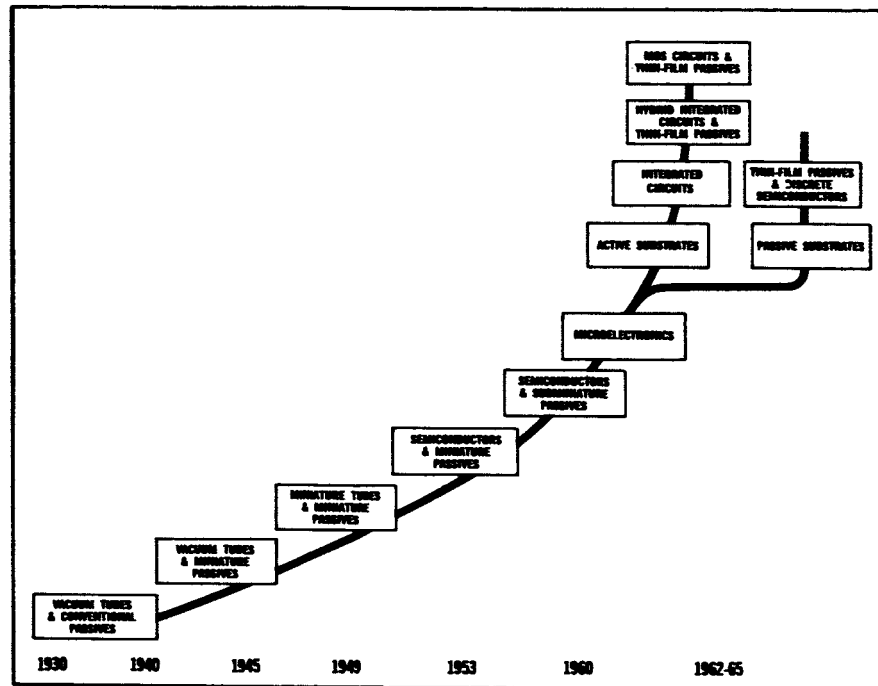


Figure 7. Evolution of Parts - Electronic Systems

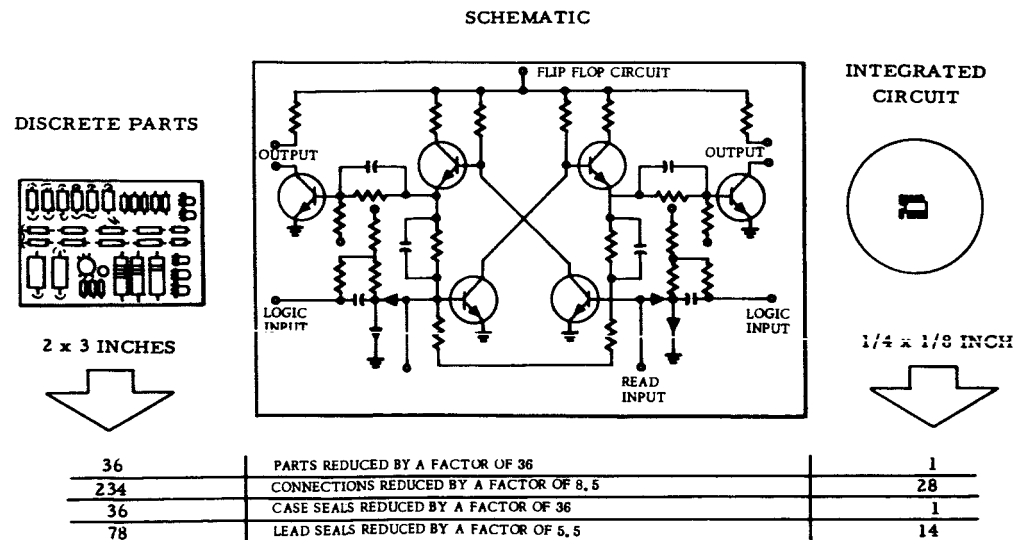
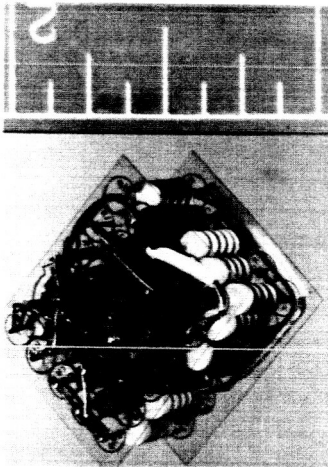
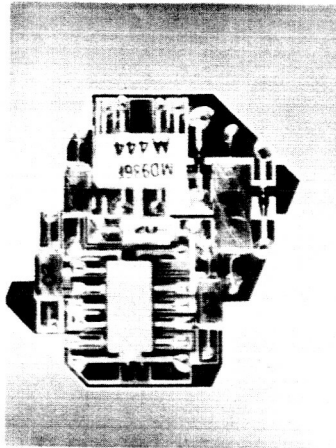


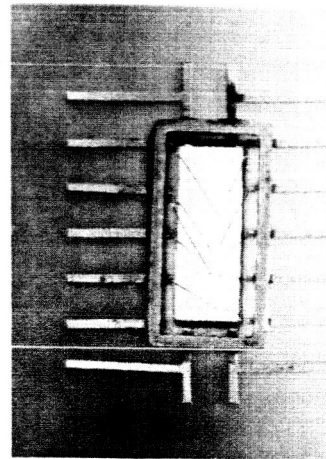
Figure 8. Reduction Obtained with Integrated Circuits



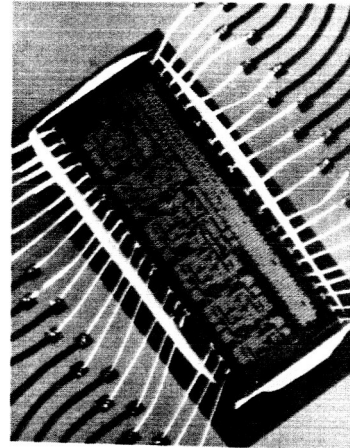
3D Packaging



Thin Film Hybrid



Silicon Integrated Circuit



Metal Oxide Semiconductor
Integrated Circuit

Figure 9. Microelectronic Techniques



With the thin film approach, some of the circuit elements (in this case the resistors) are batch fabricated as a single component. The limitations of this technology are such that many of the circuit elements must be produced as separate parts and assembled onto the thin film substrate. However, to the extent that the batch fabricated elements comprise the circuit, the number of components is reduced.

With the silicon integrated circuit technology, a sufficient assortment of active and passive elements can be provided so that a complete circuit function can be batch fabricated. With this technique virtually all digital functions and a great many linear functions can be integrated. Thus, one part can replace many parts. This marks the beginning of significant improvements in reliability, size, cost, and heat dissipation.

In the metal oxide semiconductor (MOS) integrated circuit, a further step in batch fabrication is accomplished. In the example shown 800 MOS transistors are formed in a single piece of silicon and intraconnected to form a complex multifunction. The circuit illustrated is a complete digital differential analyzer incorporating all the necessary memory logic, and register functions. MOS represents the "second generation" in microelectronics, the second large step in size, weight, power, cost and reliability improvement.

The reduction in parts count that has been effected by use of first generation silicon integrated circuits (not MOS) is illustrated in Figure 10. Here 19 circuit boards with approximately 2000 discrete element parts are replaced by 1 circuit board with 196 integrated circuit parts — a 10 to 1 reduction in parts count. The 19 discrete element circuit boards each carry an 82-pin connector. The integrated circuit board connector has 192 pins — a reduction of almost 8 to 1 in total connector pins. Comparable power reductions are obtained. These are striking reductions.

With the large scale metal oxide semiconductor array technology, as shown in Figure 11, a very large circuit function can be provided in one part. To perform the function of this one MOS circuit would require 100 conventional integrated circuits. The reduction in device leads is 1000 to 40 — a ratio of 25 to 1. Heat dissipation on the functional basis is reduced in a smaller ratio. These examples are drawn from digital circuitry but the same considerations apply to linear circuits.

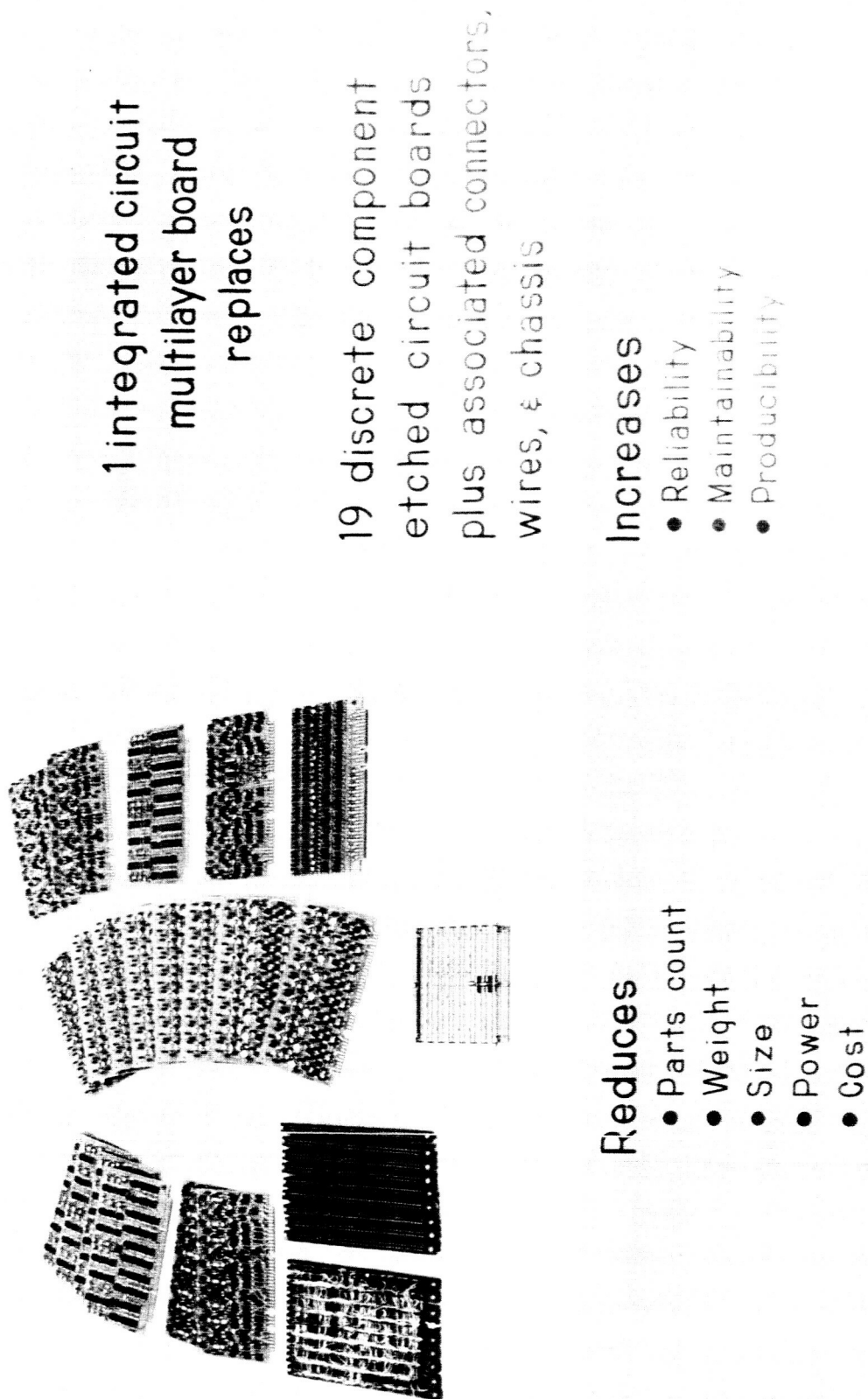
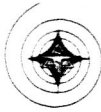


Figure 10. Microelectronics



Function

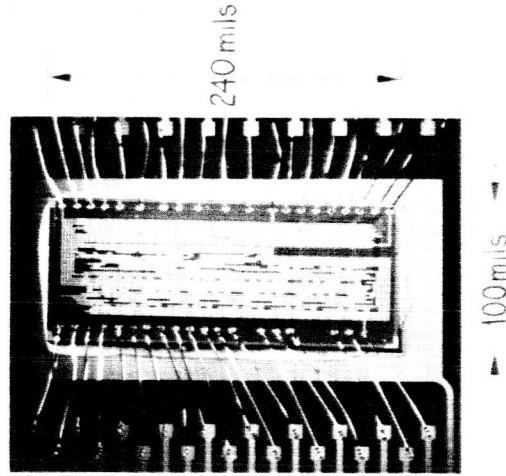
- 28-Bit Digital Integrator -- Contains 800 MOS FET's Connected in 220 Gates
- 50 to 500 KC Clock Rate

Replaces

- 100 Conventional IC Flat Packs
- 1 Multilayer Board
- 1 Board Connector

Advantages

- Low Cost
- Low Power
- Size



Digital Differential Analyzer

Figure 11. Large Scale Multifunctional Arrays



The future, or "third generation", is already beyond embryonic stages in the laboratories. At Autonetics alone, research and development are being pursued in many areas such as solid-state devices for microwave applications, solid-state micro-memories and displays, deposited waveguides and high resolution conductors, micro-layer boards compatible in size with the integrated circuitry they will carry, and new micro packaging techniques.

Of particularly significant development has been silicon-on-sapphire (SOS), a controllable, repeatable process of epitaxially "growing" high quality silicon crystals on a sapphire substrate. This Autonetics development is resulting in a great variety of exciting new microelectronic devices, unattainable by any other technique. For example, SOS makes it possible to fabricate extremely small areas (about 1 square micron) p-n junctions. These junctions, as diodes, have storage times of less than 0.5 nanosecond (5×10^{-10} seconds) and show great promise in large diode arrays for high-speed, high-bit-density memories. SOS also permits fabrication of insulated-gate, field effect transistors, employing single-crystal materials. The insulating properties of sapphire fabrication and the operation of complementary MOS devices on a common sapphire substrate, which can be in close proximity without parametric electrical paths, form extremely low-power digital circuit combinations when cascaded or paralleled. Sapphire offers, in addition to excellent dielectric and strength properties, improved thermal properties compared to silicon.

Another Autonetics development has been the planar annular varactor which opens the door for solid-state invasion into the microwave field. The planar annular varactor has a conduction path of only 3 microns, less than 100 times less than conventional devices and are therefore not susceptible to "skin effects".

The degree or sophistication of microelectronics one should use today depends on its application. Microelectronics may be categorized into three classifications: digital, radio-frequency (rf), and linear (analog). Digital systems include computers, signal converters, and other data processors. Circuit functions in these systems are pulse-driven, on-off (switching) operations and are largely repetitive and low-power. Few capacitors are used and those which are used are small in electrical and physical size. Semiconductor IC's are ideal for these digital applications.

In rf applications (radios, televisions, radar systems, etc.), capacitors are still small but relatively larger numbers are needed. Also, in contrast to digital applications, rf microelectronic requires transformers, inductors, and high-precision resistors (e.g., for gain adjustment of amplifier-type circuits common to rf applications).



Distributed and stray capacitances must be minimum. Thin films presently offer the best solution. To date, IC technology has not progressed as rapidly in the rf field as in the digital because of the difficulty of fabricating high-speed transistors. However, second-generation semi-conductor devices, novel isolation techniques, and new economical batch-produced field-effect devices are rapidly solving this problem and future rf systems will be able to exploit integrated circuitry to almost the same extent as the digital systems have been able to do.

Linear circuits are used in those electromechanical control systems (e.g., inertial navigation and flight altitude control) which interface with transducers such as gyro pick-offs, accelerometers, velocity meters (vm), servo motors, torquing coils, and voice coils. (However, digital gyro pick-offs, vm outputs, etc., are coming into greater use). The circuitry often consists of amplifiers in the dc to 100 kc frequency range with 5 kc typically the highest common frequency.

Because of the low frequency range of linear electronics, capacitors are large in value and size, generally greater than 1000 picofarads. Further, a large number is required for coupling and bypassing functions. Interface with transducers require relatively high power levels. The microelectronic packaging techniques must therefore be compatible with mounting and heat removing methods of power dissipating discrete transistors and resistors.

Despite these problems, IC's have been effectively applied to about 70% of the circuit requirements in typical electromechanical control systems. Standardized semiconductor IC's have been designed for use with adapting circuits employing discrete and thin film components, a "hybrid" approach. Through revised system techniques of grounding, power supplies, impedance levels, and information format, large capacitors and inductors have been reduced in size and number, thereby reducing power requirements. The heat-dissipation problem is further mitigated by operating power amplifiers in highly efficient switching modes.

Applications of microelectronics, both digital and linear, to computers, communications and radar systems are amply described, for example in "Proceedings of the NSI/AFS Microelectronic Conference on Application of Microelectronic Technology", December 8-9, 1965. (Further information of microelectronics may be obtained from the Autonetics Division of NAA. NASA-MSFC personnel may contact R.O. Wyne, Autonetics-Huntsville Representative, NAA.



Publications P-00075.00-0/317-3-U, Microelectronics at Autonetics, and T5-2127/3061 Microelectronics for Aerospace Applications, may be useful. A more comprehensive publication is currently being edited and will be available soon entitled, "Story of Microelectronics - First, Second, and Third Generation".

Instrument Packaging Constraints/Requirements

As a result of microminiaturization, the following can be anticipated:

- (1) Heat loads of individual instrument packages will be smaller. In the manner that 50 watt packages have become more common than 200 watt packages, 15 watt packages will become more common than 50 watt packages.
- (2) Total astrionic system heat loads will become only slightly smaller. The system will consist of more packages performing more functions.
- (3) The astrionic unit will be more dependent on forced cooling to meet higher reliability goals and to counter otherwise higher temperatures resulting from increased heat densities.
- (4) The integral coldplate packaging concept will become increasingly dominant. The integral coldplate packaging concept is one where the coldplate is a physical and usually a structural part of the instrument package and is contained within the package envelope.
- (5) Active vehicle cooling systems will be required which supply coolant to the individual instruments. The larger number of smaller heat load packages will permit series and series parallel coolant loop connections to permit the coolant to return to the vehicle ECS at the warmest possible temperature.

It will be the purpose of the state-of-the-art survey to substantiate (or refute) these postulated astrionic package constraints and requirements.

As heat densities increase, more effective means are required for transferring the heat from its point of dissipation to the package enclosure or integral coldplate. Presently, this heat transfer is predominantly done passively by conducting heat along definite thermal (metallic) paths. In some special cases, it is done actively by



recirculation of a gas within a sealed enclosure. If heat densities increase further, possible improved package-internal heat transfer methods include thermoelectric heat pumps distributed within the package (see H. Kamei, et al, "Applications of Thermoelectric Cooling to Avionic System LUR's," NEPCON, June 21, 1966) and direct exposure of active circuit elements to the vehicle supplied liquid coolant.

Electrical Heat Load Requirements

The foregoing discussion on microelectronics should indicate that heat loads, for the same functional requirements, will continually decrease. At the present pace of microelectronics, a conservative guess is that the total electrical heat load will decrease at a rate of perhaps halving every two years. But with continually increasing functional requirements and astrionic system complexity (made possible and attractive by smaller size, weight and cost and improved reliability), the total heat load may decrease more slowly, perhaps halving every 4 or 5 years. This seemingly slow improvement is dictated by economic and other factors, not technological capability.

Of course many equipments, particularly the digital circuitry type, will decrease at the much faster rate. Other equipment, such as the transmitter (output) stage of radars, telemetry, etc., which depend on transmitted power, will not decrease significantly. However, even here available techniques, such as trading off digital storage of information against transmitting information at high frequency and short duration bursts, will be used to reduce heat dissipation.

Table I shows a comparison of a modern digital computer, the D-37C computer in production for Minuteman II, with more advanced computers than can be available within the next 2 to 6 years. Heat dissipation is reduced from about 300 watts to 15 watts. It was recently found that a digital computer to perform a hypothetical space vehicle computation requirements shown by Table 6, could be built by conventional microelectronic techniques to dissipate only 12 to 15 watts. The hypothetical mission was a composite of missions studied for Standardized Space Guidance System (SSGS) having the mission phases on: (1) Prelaunch, (2) Atmospheric Ascent, (3) Exo-Atmospheric Ascent, (4) Orbital Coast, (5) Orbital Change, (6) Rendezvous, (7) De-Orbit, and (8) Re-Entry. By using a distributed logic computer system, (Reference, TS-2001/33, Systems Study for Low Power Spaceborne Computers, 5 Nov. 1965, Autonetics, Data System Division), it was found that the same computational requirements could be implemented with dissipation of only 5 to 6 watts.



Table 5. Computer Characteristics Summary

	D 37C	Advanced Computer		
		2 years	3 to 4 years	4 to 6 years
Availability	Now			
Weight	39 lb	19 lb	13 lb	9 lb
Volume (Maximum Dimensions)	0.73 cu ft 20.9 x 5.7 x 10.5 in.	0.26 cu ft 5 1/2 x 7 1/2 x 11 in.	0.13 cu ft 5 1/2 x 7 1/2 x 5 1/2 in.	0.08 cu ft 4 1/2 x 6 1/2 x 4 1/2 in.
Power	300 watts	72 watts	45 watts	15 watts
Clock Rate	345.6 kc	750 kc	750 kc 2 ϕ	750 kc 4 ϕ
Add Time	78.25 sec	4 sec	4 sec	4 sec
Memory Capacity	7222 words 24 bits	17,408 words 24 bits	17,408 words 24 bits	17,408 words 24 bits
Technology	Integrated circuits disk memory	MOS IC's, laminated ferrite memory	Polytab MOS IC's laminated ferrite memory	Reg bond MOS IC's, epitaxial ferrite memory



Table 6. GP Computer Requirements

Mission Subtask	Storage, Instructions and Constants	Operations per Mission	Seconds per Iteration	Operations per Second
Pre Launch				
1.1 Accelerometer Calibration	520	660	Not Critical	
1.2 Platform Alignment & Gyro Bias Calculation	340	540	Not Critical	
1.3 Mission Targeting	380	340	300	1
Subtotal	1240			1
Atmospheric Ascent				
2.1 IMU Mechanization	320	280	0.1	2800
2.2 Navigation Computation	290	440	0.1	4400
2.3 Steering	220	170	0.1	1700
Subtotal	830			8900
Exo-Atmospheric Ascent				
3.1 IMU Mechanization	320	280	0.1	2800
3.2 Navigation Computation	290	440	0.1	4400
3.3 Attitude Control	290	70	0.1	700
Subtotal	900			7900
Orbit Coast				
4.1 Integrate Free Fall Navigation Equations of Motion	60	1800	10	180
4.2 Orbit Determination by Smoothing and Filtering	4660	8700	10	870
4.3 Sensor Pointing	360	1930	0.33	5790
4.4 IMU Alignment and Gyro Bias Calculation by Smoothing and Filtering	80	430	Not Critical	
Subtotal	5160			6840
Orbit Change				
5.1 Set Up Rendezvous Injection	1280	1940	300	7
5.2 Set Up Midcourse Maneuver	220	8000	60	14
5.3 IMU Mechanization	320	280	0.2	1400
5.4 Navigation Computations	290	440	0.2	2200
5.5 Orbit Change Steering	470	210	0.1	2100
Subtotal	2580			5721
Rendezvous				
6.1 Rendezvous Sensor Pointing	200	1930	0.1	1930
6.2 IMU Mechanization	320	280	0.5	560
6.3 Navigation Computation	290	440	0.5	880
6.4 Rendezvous Vehicle Control	370	490	0.1	4900
Subtotal	1180			8270
De-Orbit				
7.1 Set Up De-Orbit	690	14,870	30	4961
7.2 IMU Mechanization	320	280	0.5	560
7.3 Navigation Computations	290	440	0.5	880
7.4 Optimal Estimating	2650	14,930	30	498
Subtotal	3950			2434
Re-Entry				
8.1 IMU Mechanization	320	280	1	280
8.2 Navigation Computation	290	440	1	440
8.3 Re-Entry Vehicle Control	620	1130	0.2	5650
Subtotal	1230			6370



Temperature Constraints

The reduction in power obtained by microelectronics is seldom as great as the reduction in volume and the resultant higher heat density tends to drive up the operating temperature. Typically, a size reduction in equipment design of a factor of 5 to 10 is associated with a heat reduction of 2. The problem of thermal management within a subsystem package thus becomes quite severe and is often the limiting factor in the degree of microelectronic sophistication utilized in a given design.

For example, although it is technically possible to fabricate useful power circuitry in integrated form, there are severe disadvantages in cost, size incompatibilities, and incompatibilities in the location of the collector where the heat is dissipated. Under these circumstances, it is obviously better to distribute the heat dissipation among individually packaged elements than to concentrate the heat in one device package. (However, when power circuits are operated in the switching mode, heat dissipation problem is greatly reduced. The circuitry necessary to accomplish the pulsewidth or other time base modulation is quite amenable to IC techniques).

For first generation microelectronic circuitry, a fairly narrow temperature operating range is required, about 0°C to 50°C at the device case. It is possible, however, to trade-off wider temperature ranges with additional circuitry complexity, weight, power, size, cost, etc. to some extent.

In such a manner, the operating temperature limits (or of the allowable temperature range of coolant supplied from the vehicle ECS) are flexible and are more significantly dictated by requirements of other equipment, such as batteries and electromechanical systems, including inertial platforms and gyros. These non-electronic equipment usually have temperature limitations, both high and low, for proper performance. For example, batteries are generally limited to a temperature range of 0°C to 40°C . These limits are usually dependent upon some temperature-dependent physical property such as thermal expansion or vapor pressure.

Non-operating temperature constraints sometimes impose as much constraint on the instrument internal thermal design as the normal operating requirements. One non-operating temperature constraint is thermal sterilization requirements on equipment which may impact the moon or a nearby planet. A NAA sterilization specification requires electronic parts, components, and subassemblies to be



exposed to six cycles of 135°C temperature for 60 to 92 hours per cycle. Tests have shown that many materials and assemblies cannot survive unless specifically designed for these requirements.

2.2 COMPONENT AND SUBSYSTEM REVIEW AND EVALUATION

The survey of current and advanced state-of-the-art in astrionic equipment development and associated thermal control and packaging design techniques, and thermal control components has been the major effort within this task. The survey effort has consisted of visits or contacts with important equipment manufacturers and of extensive literature survey. This survey effort is a continuing one and will extend into the next quarter.

In conjunction with the survey, a review of some of the important components of a thermal control system has been made. These are discussed in the following paragraphs and in most cases, the reviews are not considered to be complete. The review and evaluation effort is to be continued and will include all the significant components and subsystems.

2.2.1 Thermoelectric Devices

With the advent of microminaturization, coupled with the inherent advantages of thermoelectric, thermoelectrics are ideal, effective means for providing supplemental cooling or heating, whichever is required from time to time, for the modern and future astrionic units. Supplemental cooling is required when the coolant supply from the vehicle ECS is inadequate, i.e., too high in temperature than is normally desired by the particular instrument package. Supplemental heating is required when the coolant is colder than desired.

Since there are no moving parts, thermoelectrics are inherently very reliable. They are easily controlled to provide as close a temperature regulation as desired but do not have the drawback of heater controllers of a wasteful high control point temperature. They are completely and easily reversible to provide auxiliary heating which is more effective than conventional resistive electrical heaters. They do not generate audible or rf noise. Most importantly, their performance capabilities do not degrade with smaller heat load capacities or size.

This divisibility feature of thermoelectrics permits the incorporation of the provisions for supplemental cooling and heating for a given instrument package within that package itself.



Conceptually, and in practice, the best place to locate the thermoelectric elements is to insert them in the plate of the package's integral coldplate. This is illustrated by Figure 12. Typical results now obtainable with reasonable package thermal design (coolant-side thermal resistance of only 0.08 C/watt) is shown by Figure 13.

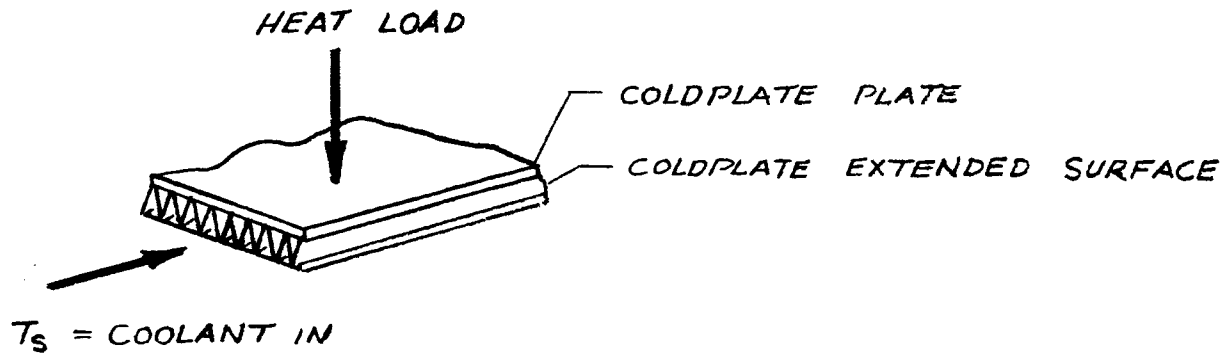
The advantages of this combination package coldplate/thermoelectric cooler are:

1. Thermal contact resistances can be minimized.
2. Extended surfaces can be integrally designed.
3. Weight and size are minimized by elimination of common structural members.
4. Coldplates are usually analyzed and designed by the same group that designs the T/E refrigerator.
5. Fabrication techniques and technology available and in use by heat exchanger manufacturers.
6. The combination is less susceptible to installation and handling damage than separate T/E modules.
7. The combination is capable of functional testing and is less subject to performance degradation due to manner of installation.
8. The heating/cooling element is closer to the temperature-controlled area.
9. Heating or cooling is applied where needed.
10. The T/E power supply circuitry may be integrated with the equipment.

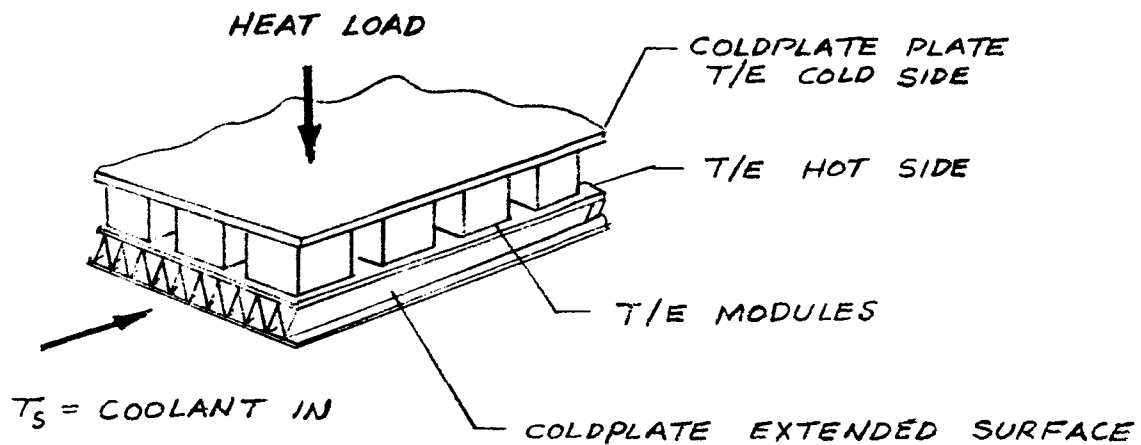
Discussions of other temperature regulation requirements or constraints will be included in subsequent reports when the survey effort is completed.

2.2.2 Joint Thermal Resistance

One important aspect to be considered in connection with electronic packages mounted on cold plates is joint thermal resistance under space vacuum condition. Since the electronic package heat load is transferred to the cold plate by conduction through the joint, it is desirable to have a low value of joint thermal



A. CONVENTIONAL COLDPLATE



B. THERMOELECTRIC COLDPLATE

Figure 12. Cross Sections of Conventional and Thermoelectric Coldplates

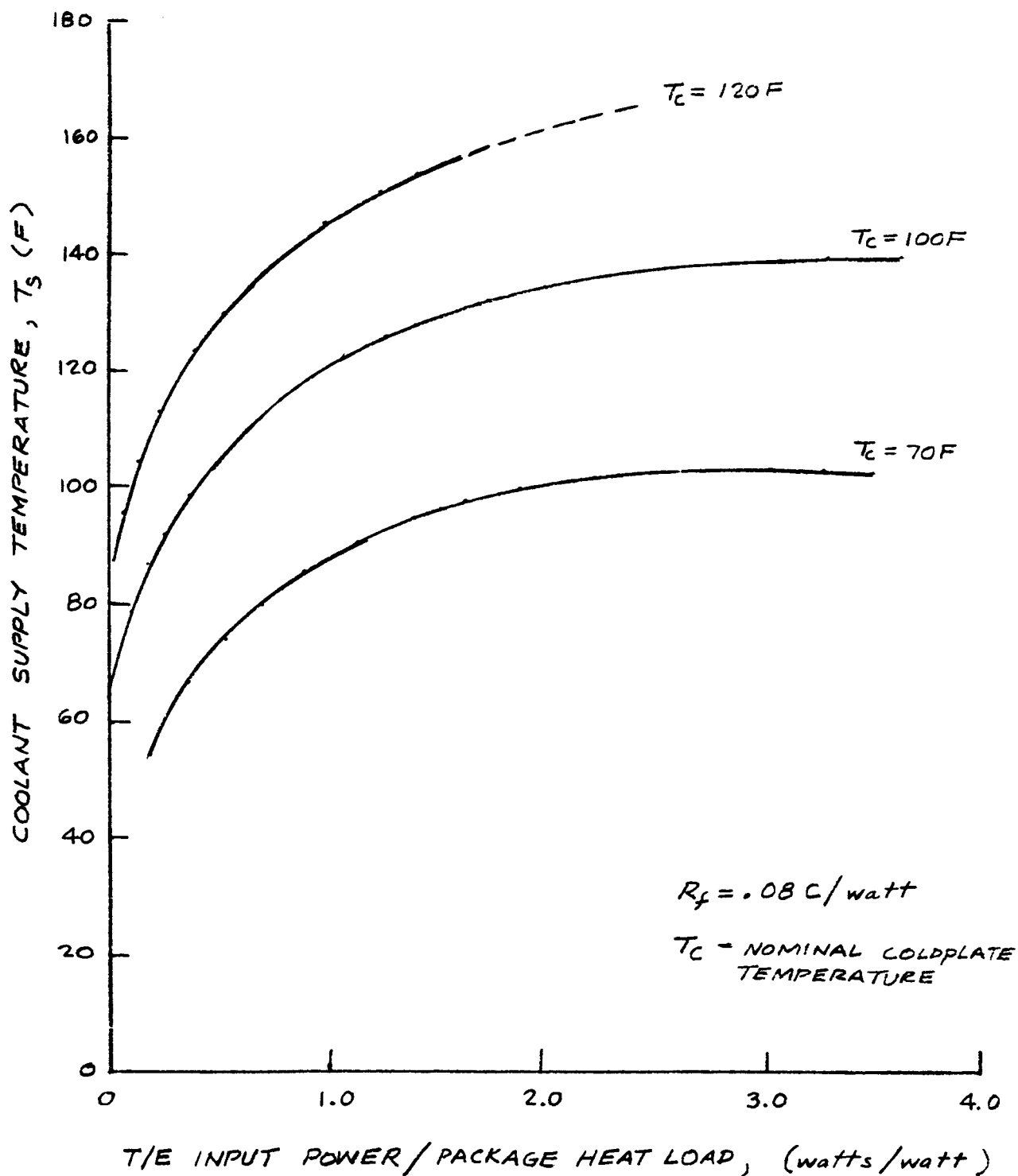


Figure 13. Coolant Temperature Versus Thermoelectric Input Power/Package Heat Load



resistance as possible to minimize the temperature differential.

A number of experimental and analytical investigations have been conducted to determine the magnitude of joint thermal resistance and the factors which influence this resistance. Although a satisfactory method for predicting the thermal performance of a joint does not appear to be developed as yet, methods for reducing joint thermal resistance have been defined on the basis of laboratory results. Such methods are concerned with the control of contact pressure, joint materials, surface finish, surface flatness, and material hardness. In addition to these controllable items, joint resistance is influenced by temperature level, heat flow rate, interstitial pressure, and interstitial fluid. Recent laboratory investigations indicate joint conductance variations up to several thousand Btu/(hr)(sq ft)(F), depending primarily on contact pressure, type of material in contact, and the absence or presence of thermal greases or crushable metals. With regard to thermal greases, only those having vapor pressures low enough for space application will be considered for possible application to this study. The amount of contact pressure which can be applied to a joint between an electronic package and a cold plate will be governed by the type of joint, the type of fastener, and the allowable load on the cold plate and the package mounting device. When typical values for the allowable contact pressure have been established, a representative range of joint thermal conductances will be chosen to determine the effect, if any, on overall cooling system design.

In the event that this study indicates a trend toward electronic packages with integral coldplates, the problem of joint thermal resistance may be minimized, particularly if it is enclosed in a pressurized container. If it appears that separate cold plates and electronic packages are a more realistic expectation for the applicable missions, joint contact area and material requirements will be specified on the basis of available information. At the present time, it appears that further research and/or detailed joint design effort will not be necessary.

2.2.3 Water Boilers

Heat exchangers which use as a heat sink the latent heat of evaporation of water (roughly 1000 Btu /lb) are useful for short duration missions, peak heat loads of short duration and when an excess or abundance of water is available.



These water boilers are usually placed downstream of the radiator or pumps in a closed loop circulating fluid system. In this location they permit the radiators to operate at peak efficiency (reject heat at the maximum temperature). The location permits automatic controls on the water boiler to operate in a zero G environment. This requires a means of transporting the liquid to a surface where it will be evaporated to cool the circulating fluid medium. Surface tension in the form of small wicks, injection thru orifices or controlled flow devices or freezing on a surface which sublimates are all suitable means of distributing the fluid to the heat transfer surfaces. These methods of distributing the fluid have given rise to several types of water boilers: - wick boilers, sublimator, force feed evaporators (forced vortex evaporators) etc.

The first two of these types of water boilers and possibly some variations are being investigated by AiResearch Mfg. Co., in a contract from NASA, Huntsville, at the present time. Our effort on these two types must necessarily be limited at the present time. However, the third type of water boiler mentioned has some information available due to tests on a possible Apollo configuration run at the Los Angeles Division of North American Aviation. This information will be parameterized. The parameterization will take into account heat rate, time of operation, temperature of operation and possibly some minor factors such as fluid pressure drop, size, etc. This should take place during the next quarter.

2.2.4 Cold Plate

Pin-fin plate-fin cold plates have been developed by North American Aviation, Inc. for the Apollo program which are being used for on-board instrument thermal control. This design is considered to be the only one which will meet the performance required in the Apollo cooling system.

Two pin-fin configurations have been investigated and these are illustrated in Figure 14. The staggered pattern configuration was selected for the Apollo application and the "U" factor and the pressure drop for various flow rates are given in Figure 15 for this configuration. The diagonal pattern gives a substantially higher overall heat transfer coefficient over the staggered pin configuration but the core pressure drop is also substantially higher. As designed for the current Apollo application, the pin-fin design

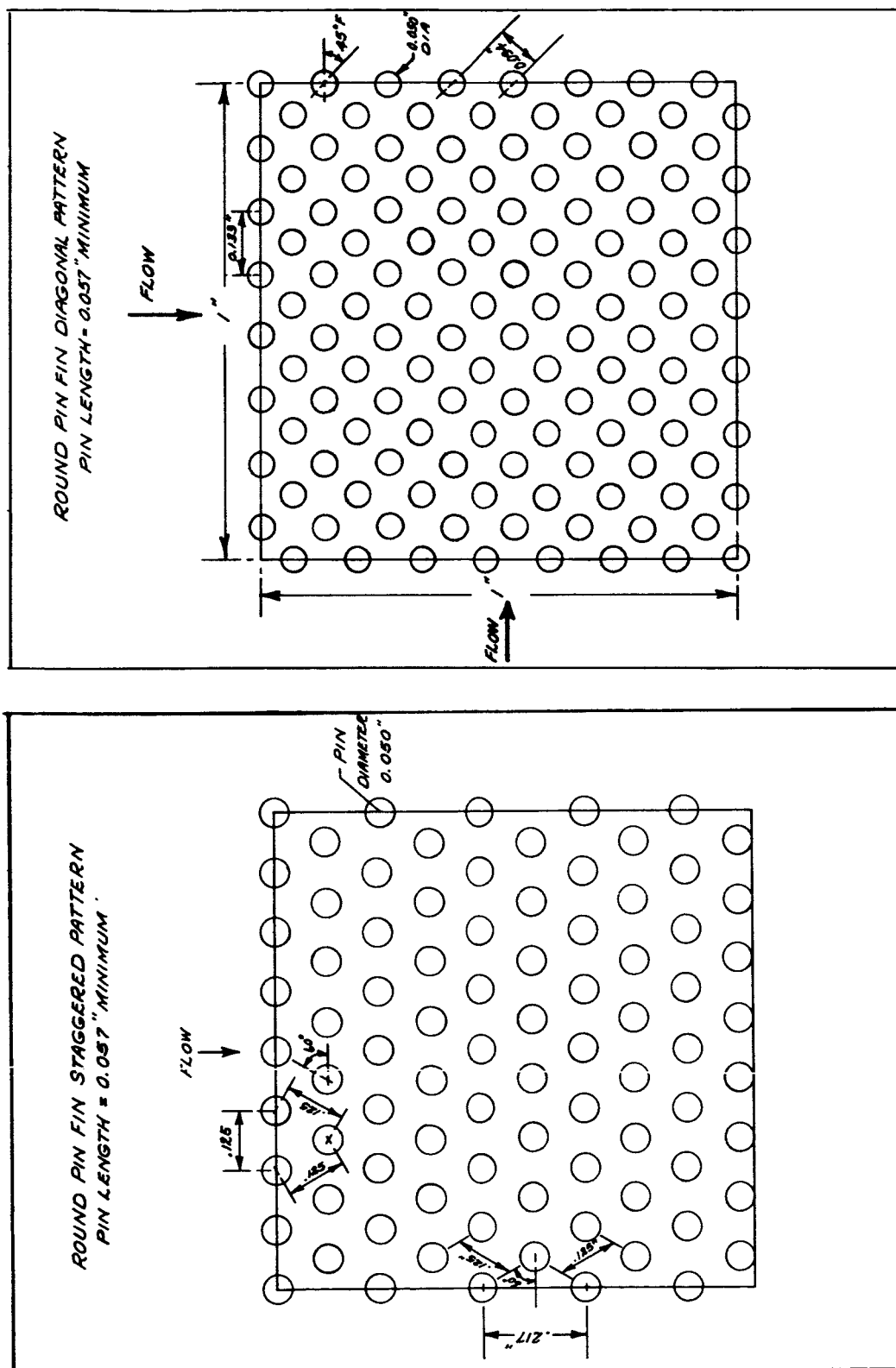


Figure 14. Pin-fin Coldplate Configurations

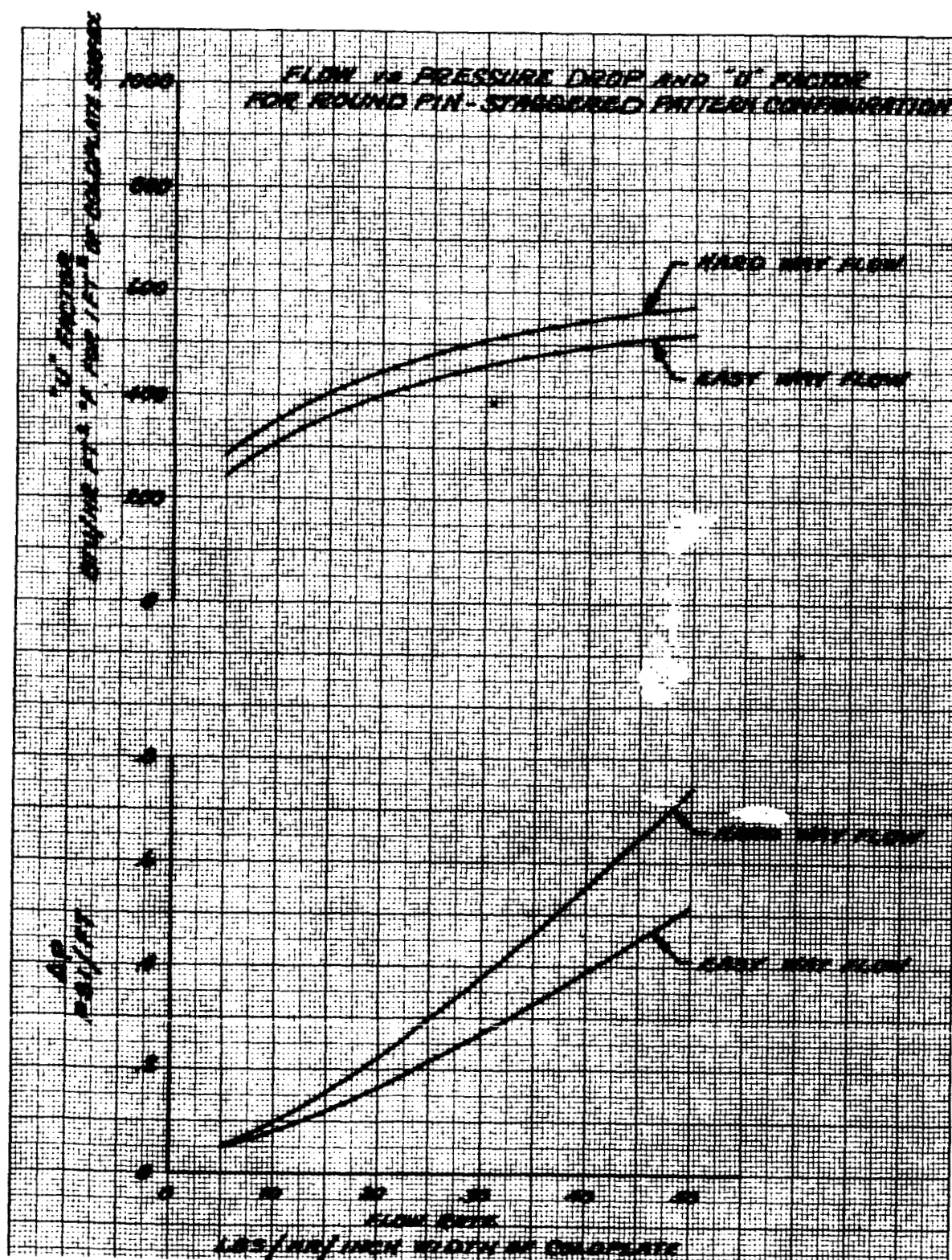


Figure 15. Pin-fin Coldplate Performance



compared most favorably over other possible fin designs, based on wet weight, pressure drop, and overall heat transfer coefficient.

The pin-fin configuration has a number of desirable features which makes this configuration suitable for possible application in the thermal control system for the Saturn V astrionic equipment. These features are:

- a) flexibility to allow various areas of the cold plate to operate at the most desired temperature by controlling the flow pattern.
- b) maximum use of pressure drop in those areas that require the highest heat transfer coefficient. This permits the optimum use of the total pressure drop allocations.
- c) complete flexibility in both pattern for equipment mounting
- d) wide variation in cold plate thickness
- e) variation in surface contour from flat to various curvatures to fit the vehicle configuration

The relative ease in achieving the desired temperature distribution and bolt hole pattern is illustrated in Figure 16. This figure shows the uniform flow distribution for a particular temperature distribution and a bolt hold arrangement.

2.2.5 Thermal Control Coatings

The surface temperature and, hence, the heat rejection capacity of a space radiator are functions of the radiator coolant inlet temperature, the absorbed incident radiation energy, and the emissivity of the radiator thermal control coating. The absorbed incident radiation energy is a function of the ratio α_s/ϵ (solar absorptivity/infrared emissivity) as well as the absolute value of emissivity. It is thus apparent that space radiator performance depends to a large degree on the choice of thermal coatings that have the proper combination of α_s and ϵ , with minimum degradation of these properties over a period of time in space.

Considerable work has been done in recent years to develop suitable coatings that will be stable in the space environment. Particular emphasis has been placed on highly reflecting white paints, since these provide the lowest effective temperatures for space radiators, cryogenic tanks, etc. Unfortunately, most white surfaces have shown considerable degradation under prolonged exposure to

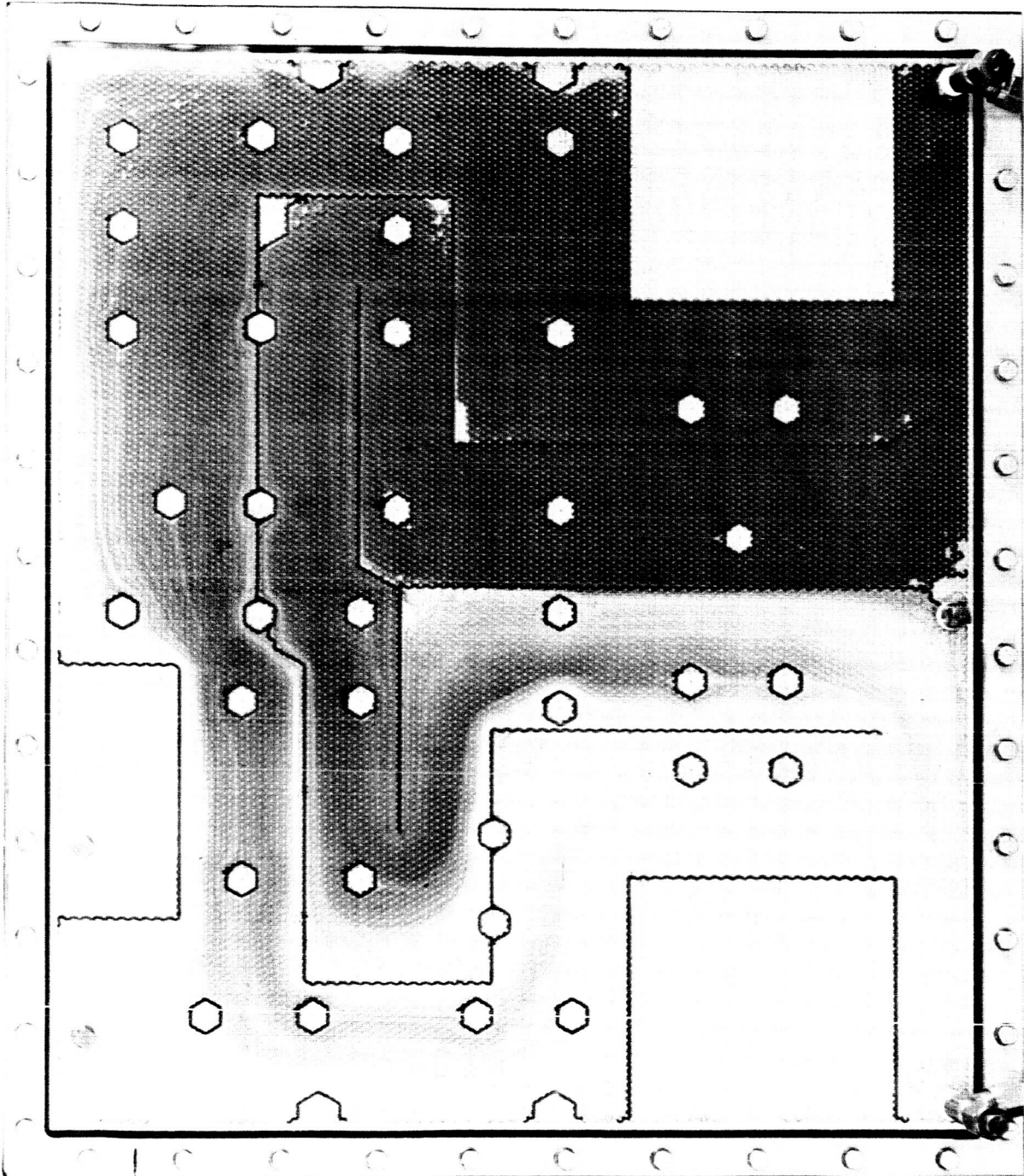


Figure 16. Pin-fin Coldplate Flow Pattern



sunlight, that is, there is a significant increase in the value of α_s . Various investigators have studied coating degradation in simulated space environments, and these studies have shown that a major cause of deterioration is ultraviolet radiation. However, true space environmental conditions have been difficult to achieve in the laboratory, and there has often been a considerable difference in test data reported by several investigators for identical test specimens. Only recently has limited actual flight data become available. This has resulted from a research program being conducted by Ames Research Center (involving both ground and flight testing) and some data recently available from Mariner-Mars.

The data available to date from the Ames program has been obtained from the first two Orbiting Solar Observatory satellites in a series designed to monitor the sun and related space phenomena. OSO-1 (S-16 Satellite) was launched on March 7, 1962, and has provided considerable long-term information since then. OSO-2 (S-17 Satellite) was launched on February 3, 1965, and has also provided considerable data since that time.

A total of six thermal coating test surfaces and one reference surface were installed on OSO-1. The first three of these were white coatings with low α_s and high ϵ . Of these, the first was a white paint which had been used previously on the Discoverer series of satellites. The second was also a white paint, and the third was a fused porcelain enamel. The last three test surfaces were coatings which possessed α_s/ϵ ratios of unity and above.

Long-term flight data from OSO-1 indicated that the two white paints, titanium dioxide in epoxy, and titanium dioxide in silicone, changed rapidly on exposure to sunlight. Neither of these paints would be satisfactory for long term thermal control. On the other hand, the white porcelain enamel exhibited very little change in thermal characteristics, although unfortunately, it is relatively difficult to apply to space vehicle surfaces. A summary of the six test coatings, their initial thermal characteristics, and degradation effects is presented in Table 7.

Inasmuch as the white paints utilized on OSO-1 did not appear satisfactory, a second group of test coatings were installed on OSO-2. A total of ten test surfaces and two black reference surfaces were installed on this vehicle, all test surfaces consisting of white coatings. Eight of the coatings were selected for possible use in thermal control of the Apollo radiators from a total of 33 candidate coatings. This selection was performed on the basis of



Table 7. Comparison of S-16 OSO Thermal Control Test Surfaces

Surface	Initial Flight Measurement			Approx. % Increase in α_s	
	α_s/ϵ	ϵ	α_s	336 Hr (2 wks)	1000 Hr
1. TiO ₂ in epoxy	0.28	0.87	0.24	60-70	90
2. TiO ₂ in silicone	0.32	0.76	0.24	30-40	50
3. White porcelain enamel	0.32	0.75	0.24	5-10	10-20
4. Aluminum powder in silicone	0.96	0.25	0.24	0	0
5. Al - SiO ₂ - Ge	3.3	0.11	0.36	5	10
6. Al - SiO ₂ - Ge - SiO ₂	2.8	0.17	0.47	0	0
7. Razor-blade reference	0.98	0.96	0.94		



considerable laboratory testing (including degradation tests) by a number of organizations under the direction of the NAA/S&ID, in conjunction with the Apollo program. A summary of the eight selected coatings and their behavior under laboratory conditions is presented in Table 8. The best coating shown in Table 8 is the first one, a zinc oxide pigment in a potassium silicate binder. This coating has a very favorable α_s/ϵ ratio and showed little degradation after 300 sun-hours of laboratory testing.

As mentioned above, OSO-2 was launched early in 1965. A recent paper describes the flight data obtained during the first 500 equivalent sun-hours of exposure. The results appear quite remarkable since they show no degradation at all for the ZnO-potassium silicate coating during this time. It should be mentioned here that comparison of results from the laboratory screening tests with the preliminary flight results indicate that laboratory tests are a very poor basis for predicting flight performances; that is, almost all the test coatings showed large discrepancies between laboratory and flight data.

Flight data are constantly being obtained from OSO-2, and this will be extremely valuable in providing further information on the long-term stability of the test coatings. In addition, NASA Ames has planned future tests for the S-57 OSO, which is to be orbited in the near future. A number of improved coatings have recently been developed by the aerospace industry. Over fifty candidate coatings have been screened by NASA Ames in order to choose the most favorable for flight testing. The selected coatings are shown in Table 9. It can be seen that these possess very desirable thermal properties, although testing so far has been somewhat limited.

Some very significant data has recently been published by JPL regarding the Mariner-Mars flight. A limited amount of emissivity testing was carried out on this spacecraft during its seven-month trip to Mars. Four test coatings were installed on the vehicle; these were chosen based upon the criteria of including a wide range of α_s/ϵ . The coatings were (1) a ZnO-potassium silicate white paint very similar to that tested on OSO-2, (2) Cat-a-lac black paint, (3) aluminum silicone paint, and (4) polished aluminum. The results for the white ZnO-potassium silicate paint were completely contradictory to the results from OSO-2, that is, the white test sample showed a continuing degradation from the beginning. This amounted to an increase of about 24 percent in the value of α_s over a period of 4-1/2 months, according to the published data. The JPL report states that "The rate of degradation is about ten times as great as found in the laboratory ultraviolet testing leading to the



Table 8. Comparison of S-17 OSO Thermal Control Test Surfaces

Surface	Initial Measurement			Approx. % Increase in α_s After 300 hr
	α_s	ϵ	α_s/ϵ	
1. ZnO in potassium silicate	0.147	0.925	0.159	8
2. Synthetic spodumene in sodium silicate	0.142	0.878	0.162	10
3. Zirconium silicate in potassium silicate	0.100	0.871	0.115	65
4. Zircon in potassium silicate	0.09	0.907	0.206	106
5. TiO ₂ in silicone	0.129	0.862	0.150	40
6. ZnO in silicone resin	0.158	0.888	0.178	16
7. Cr-Ni Spinel - SnO ₂ , phosphate and silicate bonded	0.197	0.947	0.208	7
8. ZnO in resin	0.184	0.867	0.212	12



Table 9. Test Surfaces Selected for S-57 OSO

Surface	Function	α_s	ϵ	α_s/ϵ	Source
1. Lithium alum. silicate in potassium silicate	White solar reflector	0.10	0.89	0.11	Lockheed
2. Zinc oxide in potassium silicate	White solar reflector	0.12	0.88	0.13	Marshall SFC
3. Zinc oxide in methyl silicone	White solar reflector	0.14	0.88	0.16	IIT Research Institute
4. Zinc oxide in silicate binder	White solar reflector	0.18	0.89	0.20	McDonnell
5. Titanium dioxide in silicone	Flight-test comparison	0.24	0.76	0.32	IIT Research Institute
6. Chemical conversion coating on aluminum	Solar concentrator	0.12	0.30	0.40	Boeing
7. Iron oxide on gold	Solar absorber	0.86	0.11	7.6	AF Materials Lab
8. Manganese black	Solar absorber	0.76	0.13	6.0	Nat'l Phys. Lab. Israel
9. Polyvinyl chloride	Lab simulation studies	0.20	0.47	0.42	Ames Research Center
10. Chromium black	Earth-albedo meas.	0.89	0.30	3.0	Nat'l Phys. Lab. Israel
11. Parsons black	Total heat-flux meas.	0.98	0.97	1.01	Ames Research Center
12. Razor blades	Stable reference	0.98	0.97	1.01	Ames Research Center



selection of the sample. Subsequent tests of ultraviolet degradation on two specimens prepared at the same time as the flight samples have shown rates similar to the flight data. This gives rise to speculation that the properties from batch to batch vary widely." The full significance of the above statement is subject to interpretation; however, if the test data from Mariner-Mars is valid, then the problem of white radiator coatings seems far from resolved, even though OSO-2 data indicates complete reliability.

One serious problem area that continues to exist with regard to white temperature control coatings (perhaps with regard to all temperature control coatings) is the behavior of such coatings when subjected to prolonged nuclear bombardment from the sun. Although considerable laboratory testing has been conducted in recent years in order to determine coating reliability, this has been almost exclusively in the area of ultraviolet testing. Only recently has nuclear testing been done, and all test results seem to indicate a serious degradation effect. Bombardment by low-energy protons seems to be extremely harmful, and tests conducted at S&ID showed that the ZnO-potassium silicate white radiator coating suffered slight to severe yellowing effects depending upon radiation intensity. A major difficulty in evaluating such tests is the lack of knowledge existing relative to the actual nuclear radiation environment existing in space. It would be extremely desirable that such an environment be determined as soon as possible (preferably from flight data).

To summarize, the following conclusions can be made:

1. Laboratory tests have indicated that a ZnO-potassium silicate white paint shows very little degradation under ultraviolet exposure.
2. Flight data from OSO-2 also indicates that a ZnO-potassium silicate paint is relatively unaffected by the space environment.
3. Flight data from Mariner-Mars is completely contradictory to the data from OSO-2, and indicates definite degradation of the ZnO-potassium silicate paint in a space environment. Admittedly, the Mariner-Mars emissivity tests were not highly sophisticated. It is not now certain whether the degradation occurred because of ultraviolet irradiation, nuclear bombardment, or possibly coating application techniques. However, this data does point out a definite need for further investigation.



4. Nuclear bombardment, especially low-energy protons, presents a potentially serious degradation problem not only to the radiator coatings, but to vehicle coatings. A major difficulty here is the lack of information relative to the actual radiation in space. Considerable investigation is needed in this area, both in defining the environment and in obtaining laboratory and flight test data.

It should also be noted that the effort to develop thermal control coatings is continuing. Of particular interest is the objective of producing a coating having an α_s/ϵ ratio significantly lower than any of the formulations listed in the above tables. A major aerospace company has indicated successful development of such a coating, which is being referred to as an optical solar reflector. Further discussion on this will be made in subsequent report as more information becomes available.

2.2.6 Space Radiator Freezing Control Methods

The heat loads may not be uniform and indeed may reach very low values during a "powered down" condition. Under these conditions the radiators used for a "long flight" may encounter problems of freezing. This is also true if some fixed favorable orientation to the sun becomes necessary. To prevent freezing of the radiator fluid or the use of excessive pumping power, several approaches that may be used are listed.

1. Use of low temperature fluids which will not freeze or use excessive pumping power.
2. Control by surface finish or coating
3. Radiator area control:
 - a. Partial freezing of radiator
4. Effectively reduce radiator surface area by:
 - a. Taking care of peak loads by use of capacitance (water boilers).



- b. Interposition of reflective solid members, such as rotating disks, fans, venetian blinds, roller shades, etc.
 - c. Interposition of reflective liquid members liquid metal filing under glass, or slurries which are non-adhering.
 - d. Interposition of a reflective or absorptive particle dispersion cloud dispersion or electrostatic transfer of solid particles.
 - e. Withdrawal of high emissivity liquids from shining surfaces, clear, opaque or slurries.
5. Maintaining heat load by:
- a. Dummy electrical heat loads.
 - b. Getting energy from some high energy source such as reactor or isotope power source.
 - c. Transferring heat from a high temperature heat source or radiator.
 - d. Reflectors to increase solar or terrestrial heat loads.

From those listed, the proper combination of the coolant fluid and the radiator surface finish or coating is the simplest approach to the prevention of radiator freezing. However, it may not be possible to achieve the desired combination. The selection of the coolant fluid is made on the basis of its overall merit which does take into account the freezing temperature. Likewise, the surface finish is selected on the basis of its overall suitability. Thus, there may be conditions when the combination alone may not be adequate. In these situations, the other approaches would be considered as auxiliary means to help prevent freezing.

In the following discussion, the survey of low temperature fluids, radiator area control and interposition devices are covered. The various means for maintaining heat load will be discussed in subsequent report.



2.2.7 Low Temperature Coolants

In establishing the α/ϵ ratio, one of the most important factors is the freezing or congealing temperature of the fluid. It follows that by using coolants with better low temperature properties plain radiators may operate over a much wider range of conditions. It may eliminate the necessity of heaters, mechanical controls, specific solar orientations; unfavorable α/ϵ ratios, peak load devices (water boilers) etc., to prevent freezing or congealing. Generally speaking, most organic fluids have only $1/3$ to $1/2$ the heat capacity per unit volume of water. Many however, have all the desirable electrical characteristics and have low freezing temperatures. Thus, an examination of various organic fluids which might be suitable for cooling was initiated.

There are a number of organic fluids which have very low freezing (or congealing) temperatures. At somewhat higher temperatures, their viscosities approach the values customarily associated with conventional liquids. The boiling temperature, if it is low, will require the cooling system to operate at fairly high pressure. A problem exists however, due to minute leakages. This leakage will be proportional to between 0.5 and 1.0 power of the internal pressure. If the fluid is to be used in direct contact with electronic equipment, the equipment and containers have to be designed to withstand high pressures. Generally speaking, it is desirable to keep the pressure down unless exceptional care is taken to design for the pressure and to find and eliminate minute leaks.

To properly evaluate each fluid as an electronic equipment coolant, a number of fluid properties must be considered. The most important are: density, specific heat, thermal conductivity, vapor pressure, viscosity. Also, other important considerations are the temperatures at which chemical breakdown takes place, corrosion characteristics, dielectric characteristics, and toxicity. Other characteristics such as the triple points, critical pressure, and temperature, etc., are helpful in the evaluation.

Examination of other fluids which may have some of the required properties was initiated. A cursory examination of many chemical compounds, mixtures, and solutions was made to reduce the list to those which might have desirable properties. Also, pure compounds were included since they have certain advantages such as: informity of properties, greater stability, of being easy to check and generally more "fool proof". On the basis of cursory examinations,



fifty compounds were selected as having desirable properties. Also, pure compounds were included since they have certain advantages such as: informity of properties, greater stability, of being easy to check and generally more "fool proof". These are listed in Table 10. Half of these compounds (those shown with an asterisk) are bulk industrial chemicals. For some of these bulk chemicals, physical properties are well known, but for most cases, very little data are available.

The compounds listed cover a fairly large range of freezing temperatures and in Table 10 they are listed in this order. For some compounds the freezing temperature has been determined by only one investigation so there is a possibility of error.

Figure 17, which gives the freezing and boiling temperatures (at 14.7 psia) of the listed compounds, shows the general trend of values. Certain other common substances (oxygen, nitrogen, carbon dioxide and water) have been included for comparative purposes. Lines extending upward from several compounds show a range of values up to the critical temperature of the particular compound. A diagonal line of equal freezing and 14.7 psia boiling point temperatures serves as a means of establishing the most promising compounds, those farthest from the line being the most promising. It can be noted, that in general for the most promising compounds, the boiling temperature is around 2.5 times the freezing temperature and that the critical temperature is around 1.6 times the boiling temperature.

2.2.8 Radiator Area Control

One method attractive from a weight standpoint but unattractive from a controls standpoint is the shutting off of unneeded radiator capacity. The unused radiator is allowed to freeze. If conditions demand the reactivation of the radiator, the attitude of the spacecraft can be positioned to expose the frozen radiator to direct solar radiation. As much as 30 minutes or even more could be required for thawing pure water in a radiator. This time could be reduced to less than a half with a glycol or alcohol water solution. The amount of reaction control system fuel to orient the ship could be as little as one pound per orientation, or even less. Since only a few orientations would be needed, this is perhaps most attractive from a weight standpoint provided, of course, that a specific attitude for thawing could be tolerated. This would prove beneficial for large electronic equipment radiator areas, probably in connection with an overall thermal system.



Table 10. Possible Organic Coolants

Organic Compound	Freezing (°F)	Boiling (°F) @ 14.7 psia	Molecular Weight
1. ● PROPANE	-310°	- 44°	44
2. 1 BUTENE	-301.6°	+ 20.7°	56.10
3. * PROPENE (Propylene)	-301.3°	- 54°	42.08
4. ORTHOVANADIC ACID (CH ₃) ₂ CHO ₃ VO	-292°	+289.4°	243.9
5. 2 PENTENE cis	-288.4°	+100°	70.13
6. 2 PENTANETHIOL	-272.2°	+235°	104.21
7. ● BUTANE, 2 METHYL (iso pentane)	-265°	+ 86°	72.15
8. TRIMETHYL BORON	-259°	- 4°	55.9
9. * DI CHLORO DI FLURO METHANE (freon 12)	-256°	- 18°	120.92
10. ● VINYL CHLORIDE	-255°	+ 7°	62.5
11. n PROPYL FLORIDE	-254°	+ 28°	62.09
12. ● PROPANE, 2 METHYL (iso butane)	-254°	+ 11°	58.12
13. 1 BUTENE, 2, 3 DIMETHYL	-251.4°	+132.8°	84.16
14. DI METHYL SILANE	-247°	+ 67.8°	60.17
15. * 2-METHYL PENTANE - 1 pure	-244.5°	+140.7°	86.17
16. 1-PENTENE, 4 METHYL	-242.5°	+128.5°	84.16
17. * BUTYLENE OXIDE	-238°	+14.6°	72.11
18. 2 HEXAMETHIOL	-232.6°	+284.0°	118.28
19. 2-HEXENE cis	-230.8°	+154.5°	84.16
20. ETHYL CYCLOBUTANE	-225.3°	+162.4°	84.16
21. * METHYL CYCLOPENTANE	-220.6°	+161.6°	84.16
22. ETHYL CYCLO PENTANE	-216.1°	+218.6°	98.19
23. * ALLYL CHLORIDE	-213°	+112°	76.5
24. * 2 ETHYL HEXYL CHLORIDE	-211°	+343.4°	148.67
25. ● VINYL ISOBUTYL ETHER	-206.1	+181.4°	100.16
26. * ALLYL ALCOHOL	-200°	+205°	58
27. 3 OCTENE cis	-196.0°	+253°	111.2
28. * CYCLO HEXYL METHANE	-195°	+212°	98.18
29. ● 1 PROPANOL (n propyl alcohol)	-195.5°	+205.7°	60.9
30. * 2-ETHYL HEXOIC ACID	-180°	+440°	144
31. * 3-METHYL-1-BUTANOL (iso amyl alcohol)	-178.6°	+267.5°	88.15
32. * 2 ETHYL BUTANOL	-173.8°	+296.6°	102.18
33. ● ETHANOL (ethyl alcohol)	-173°	+173°	46.07
34. 5-DECENE cis	-169.5°	+337°	140.26
35. TOLUENE, nFLURO	-167.5°	+240°	110.13
36. * 4 VINYL CYCLO HEXENE-1 pure	-166°	+276°	108
37. ● TETRA (2-ETHYL BUTYL) ORTHOSILICATE	-148°	+460.4°	432.76
38. * ISO OCTANOL	-148°	+366.8°	130.23
39. CAPROALDEHYDE ETHYL	-148°	+326°	128.21
40. ETHYL BUTYL ACETATE	-148°	+323°	144.21
41. ● PRIMARY AMYL ACETATE	-148°	+294.8°	130.19
42. ● CUMENE	-142°	+306°	120
43. 2 ETHYL HEXYL ETHER	-139°	+516°	242.43
44. * ETHYL BENZENE	-137°	+276°	106.16
45. BUTYL VALERATE	-135°	+365°	158.28
46. ● n BUTYL ETHER	-122°	+287°	130.23
47. DI BUTYL MELATE	-121°	+536°	228.28
48. AMYL BENZENE	-108.7°	+395°	148.24
49. GLYCEROL TRI ACETATE	-108.4°	+497°	218.20
50. TRI BUTYRIN GYLCOL	-103°	+597°	302.36

* BULK INDUSTRIAL CHEMICALS

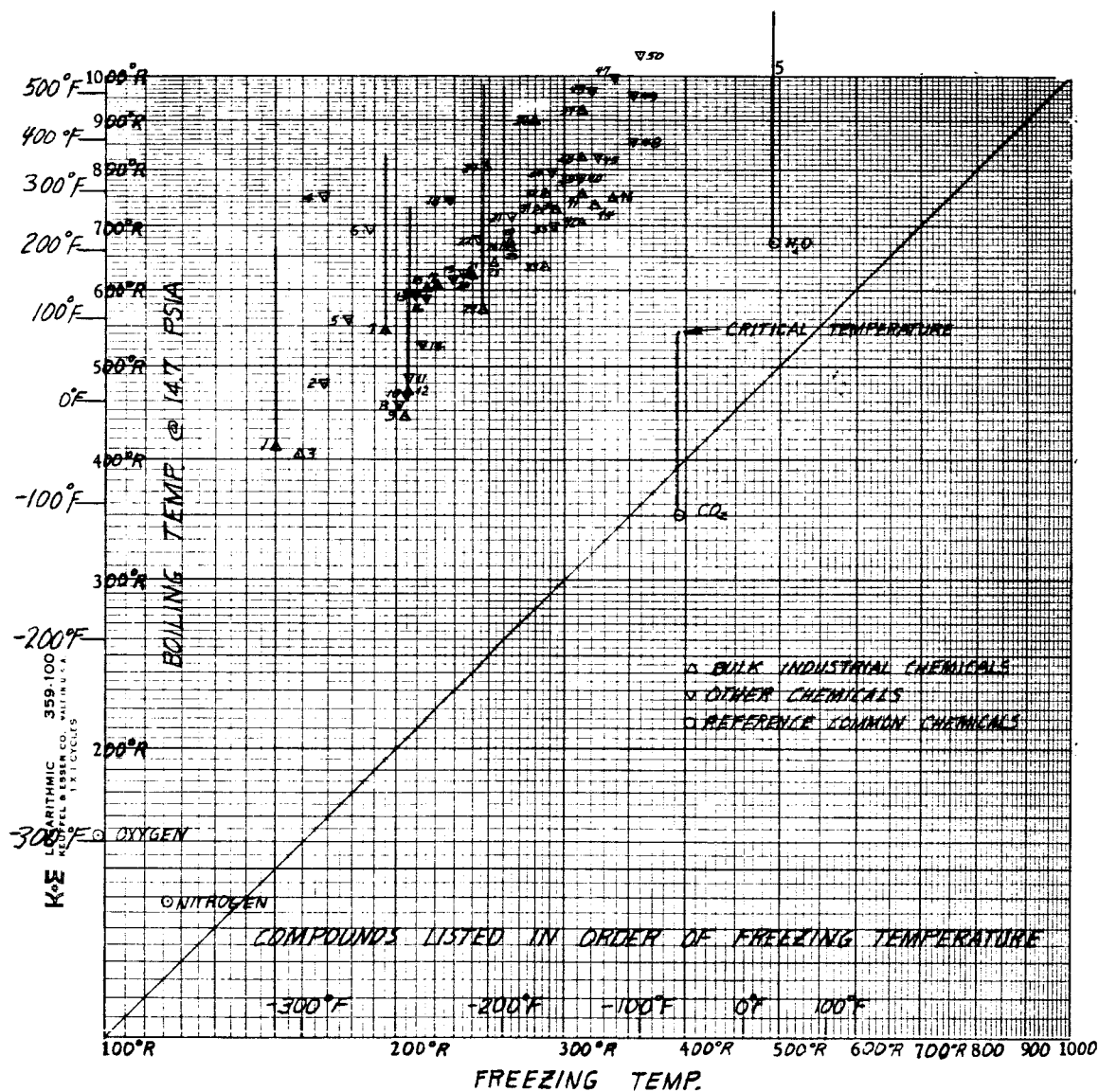


Figure 17. Compounds for Low Temperature Operation



2.2.9 Interposition Devices

In space, extremely light interposition devices could serve as an effective control of radiating area. This in effect serves as a control of freezing of the heat transport fluid. One layer of superinsulation (NRC-2) which weighs .002 lb/sq ft would enable water to be used in a radiator whose heat rejection is as low as 4.5 Btu/(hr) (sq ft). This corresponds to an equilibrium temperature of -234F. Four layers of superinsulation (.008 lb/sq ft) would enable water to be used in a radiator whose heat rejection was as low as 1.125 Btu/(hr) (sq ft). This corresponds to an equilibrium temperature of -300F. The interposition devices serve to reduce the effective emissivity by substituting the emissivity of the very reflective superinsulation ($\epsilon = .043$) for that of the radiator ($\epsilon > .90$).

A number of mechanical means exist to interposition as a reflective layer between the radiator and space such as rotating disks, "Japanese" fans, Venetian blinds and roller shades. During launch severe vibrations, g loads and aerodynamic forces as well as high temperature act on these mechanical devices. Designing for these conditions and for operation in space adds weight and complexity. If these mechanical means are completely automatic they appear to be unattractive in any size. If any of these devices could be applied by an astronaut after launch into space, some of the severe loads could be minimized and the design simplified accordingly.

The interposition of a liquid with properties of changing the α/ϵ rates of the radiator surface would accomplish the controls necessary to prevent freezing of the radiator fluid. The problems involved in such an operation appear almost insurmountable. The fluid must be able to be inserted and withdrawn in zero " g " conditions. The glass cover plate must be light and meteoroid resistant. Allowances for fluid expansion must be provided unless the fluid has an ultra low vapor pressure.

Another possibility, if it can be made to work, is to adhere a number of charged particles to the radiator and either add to or withdraw particles from the surface electrostatically. If the particles have the opposite characteristics to the surface (particularly if they are shiny and the radiator surface black) this will be an easy means to control the α/ϵ ratio on the radiator surface and freezing can be easily eliminated. Fixing the particles to retain their charge and establishing the method of charging the radiator and some other surface appear to be the major problems.



2.3 PARAMETRIC STUDY AND TRADE-OFF ANALYSIS

Parametric study was initiated in several areas which are basic to a thermal control system. The parametric effort is directed toward providing data in easy to use form which can be readily used for either performance evaluation or comparative evaluation in the selection of components or processes. This provides a rapid means for the selection and sizing of the various components which can then be analyzed more in detail.

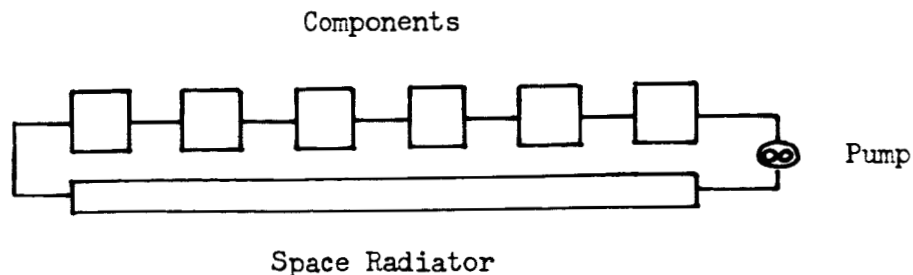
Those areas in which some significant results have been obtained are discussed in the following paragraphs. The parametric study is a continuing effort and it is expected that many areas will be investigated.

2.3.1 Manifolding

Simplicity is the reason for use of a single cooling system even when there is a large number of remote electronic components and systems. The fluid in the cooling system removes the heat from the individual components and deposits it in a heat sink. The main lines through which the fluid circulates (manifolding) may take a number of different configurations and thus needs to be investigated. The weight of the lines, contained fluid and chargeable power loss may, in some instances, be an appreciable value as shown in the preliminary investigation of two idealized types, Figure 18.

For large manifolding configurations, the flow usually is laminar. Since only in large sizes does manifolding have an appreciable penalty, investigations of manifolding can be confined to the laminar region. In the laminar flow region, there is little weight advantage in stepping the manifold as flow along the manifold decreases.

The individual components may be arranged along the flow path in a series arrangement as shown below:



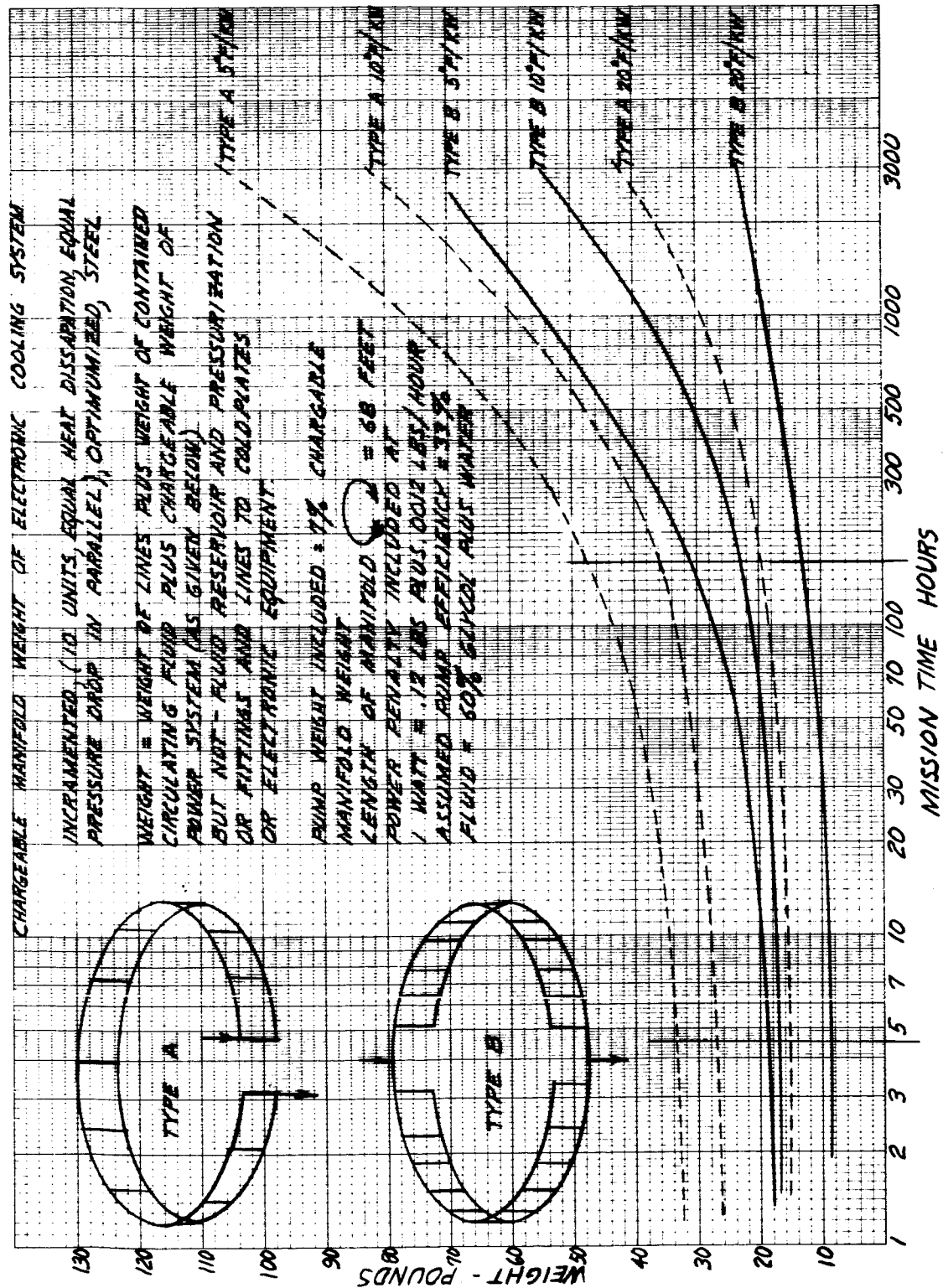
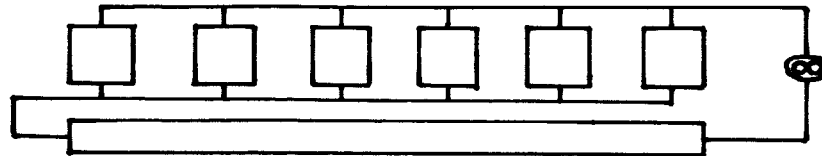


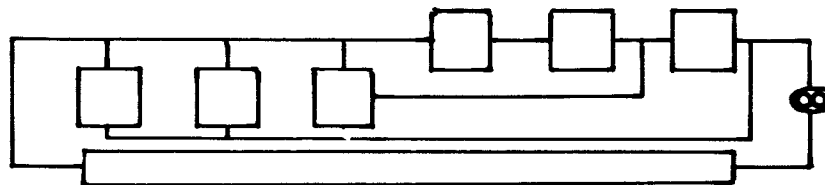
Figure 18. Manifold Weight Versus Mission Time



or in a parallel arrangement as shown below:



or some combination of both:



For the basic manifold types, the parallel and series, the temperature variation along the flow path is shown in pictorial form in Figure 19. This figure also shows some of the many possible manifold configurations when the electronic equipment is positioned around a cylindrical surface. If the flow to the individual pieces of equipment is in parallel with other pieces of equipment, what happens in other pieces of electronic equipment has little effect on the temperature environment of the particular piece of equipment. The flow in the manifold is greater than for a series arrangement, requiring larger line size and more contained liquid. The basic types can thus be characterized as parallel arrangements with better temperature controls, and series arrangements with better weight and size characteristics. Combinations can be used to combine the best features of each. In the series arrangement, it is also possible to position radiators along the flow path much as intercoolers are placed in engine fluid circuits. This is particularly desirable if the transport fluid will not freeze.

The chargeable weight, tube weight plus fluid weight plus power penalty, for various tube sizes is optimum at different lengths of operation. These curves for different tube sizes and a particular configuration are shown in Figure 20. The optimum, if there is no restriction on tube size or pump size, is shown in a tangent line to the curves for tube sizes. This optimum for different loadings and two different configurations is shown in Figure 20. Since tube is redrawn to the standard and special sizes suitable for manifolding the optimum curve can be easily approached.

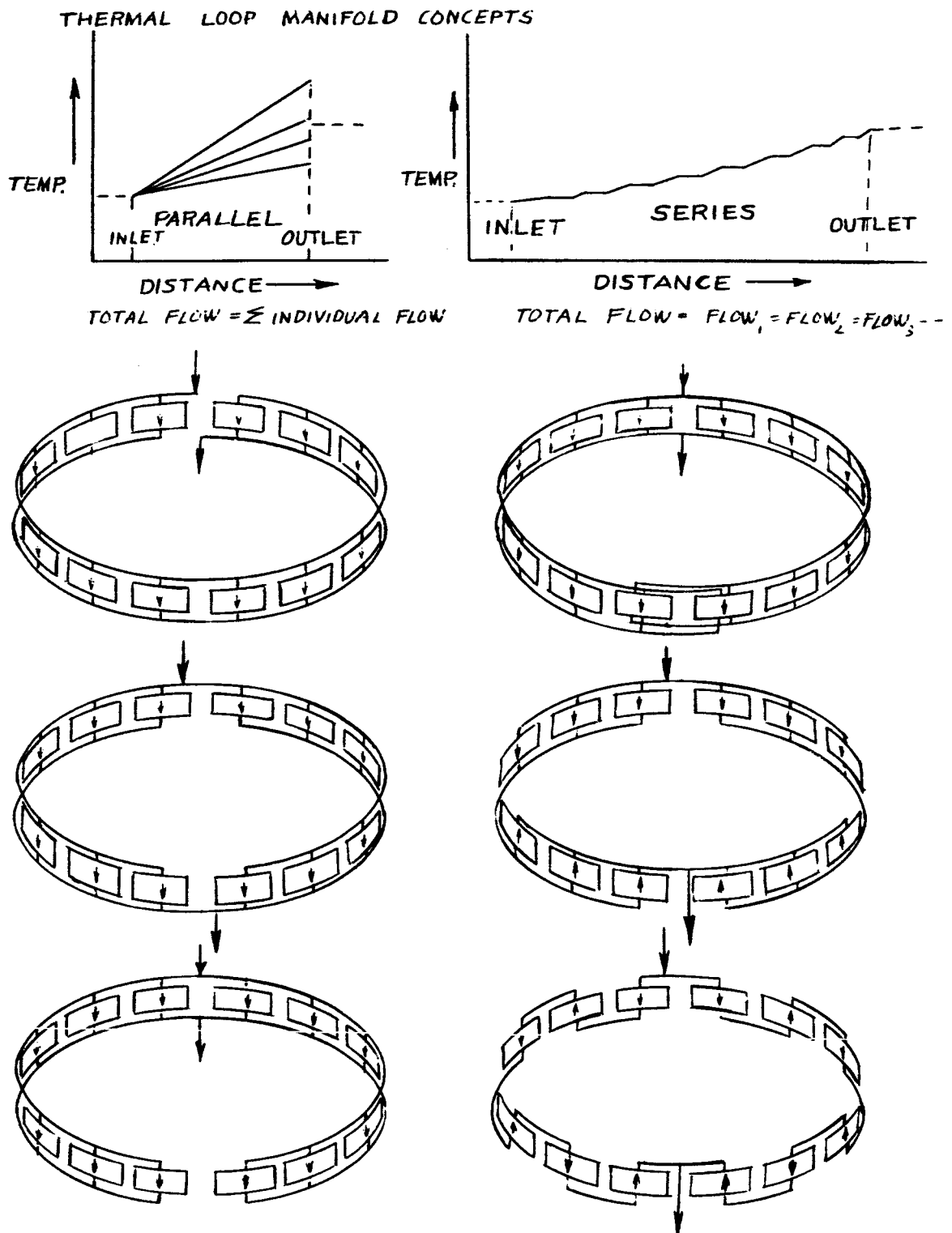


Figure 19. Manifolding Concepts

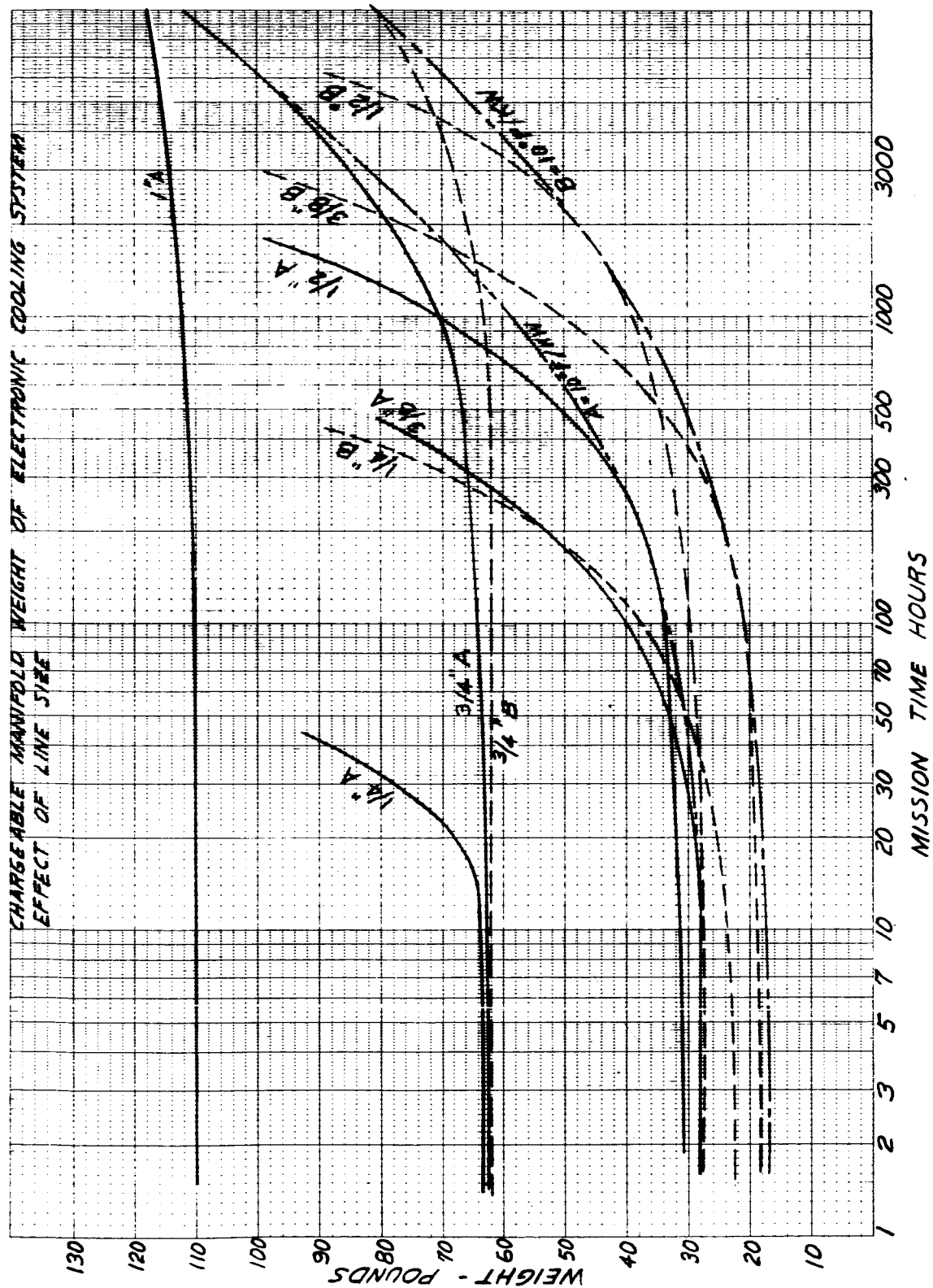


Figure 20. Manifold Weight Versus Mission Time



Though exact pump size is not usually achieved by matching line to pump size and equipment restriction, the system very closely approaches the optimization lines. Pump size and equipment restrictions (pressure drop and flow requirements) fix for the required flow, plus a margin for reliability, the permissible pressure drop in the manifold. Various configurations can then be calculated to give the required pressure drop and the one which is suitable and which has the lowest chargeable weight is selected.

The analysis of manifolding without specific configuration and power level is very difficult but some approximations and parameterization will be made.

2.3.2 Space Radiator Design

For the purpose of establishing space radiator requirements within sufficient accuracy for the parametric study of cooling systems, radiator performance data available from the Apollo program has been used. This performance is summarized in Figure 21 for a range of radiator inlet temperatures and with absorbed energy as a parameter. Absorbed energy is that portion of the incident thermal radiation which is not reflected and is dependent on the values of solar absorptivity and infrared emissivity of the radiator thermal control coating. The radiator heat rejection rates represent energy lost by the coolant flowing through the radiator, and they are added to the absorbed energy to arrive at total radiator heat rejection. It is to be noted that the data of Figure 21 are based on a value of 0.92 for the infrared emissivity of the radiator coating.

The data shown in Figure 21 were obtained with the aid of a digital computer program which is described in S&ID Report 63-74. The program follows the basic theory presented in ASD technical reports 61-30 (Part I and Part II) and 62-567; and the calculated performance map represents the capacity of a specific design. However, a parametric study of radiator configurations has shown that radiator performance is determined primarily by surface properties (solar absorptivity and infrared emissivity). Other parameters, such as tube diameter, wall thickness, tube spacing, fin thickness, coolant flow rate, and coolant properties, have been found to exert relatively minor influences. Therefore, the radiator performance map of Figure 21 is considered to be applicable to a number of radiator configurations provided certain limitations are observed. These limitations are a surface emissivity of 0.92, a tube spacing within the range of 4 to 6 inches, and a coolant flow rate of 100 lb/hr for a radiator with a 30 square foot area. With these restrictions in mind, Figure 21 and other curves derived from it can be used to estimate required radiator areas for a parametric cooling systems study. Of course, once a specific system has been selected for a

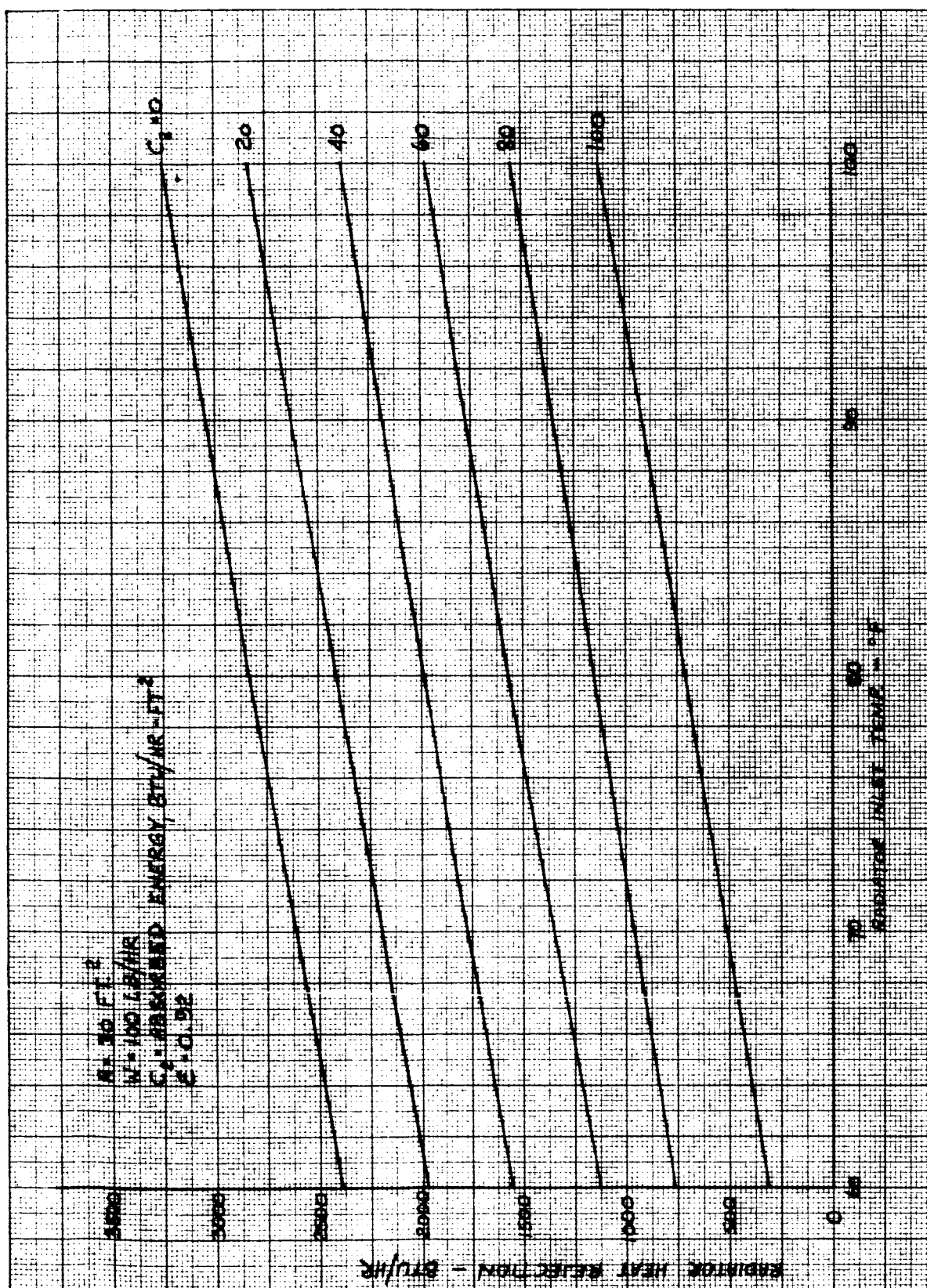


Figure 21. Space Radiator Performance



more detailed analysis, the performance of the radiator configuration chosen for that system can be calculated with more precision through the use of the computer program.

To transform the performance map of Figure 21 into a form suitable for a parametric study and to permit an evaluation of the effect of variation in surface coating emissivity on radiator performance, the following procedure was used.

For a radiator inlet temperature of 80°F and an absorbed energy rate of 40 Btu/(hr)(sq ft), Figure 21 indicates a radiator heat rejection of 2000 Btu/hr. Since radiator area = 30 square feet, the unit area heat rejection rate, q , is

$$q = \frac{2000 \text{ Btu/hr}}{30 \text{ sq ft}} = 66.6 \text{ Btu/(hr)(sq ft)}$$

Total unit area heat rejection, q_R , is the sum of q and the absorbed energy, C_2 .

$$q_R = q + C_2 = 66.6 + 40 = 106.6 \text{ Btu/(hr)(sq ft)}$$

Average radiator surface temperature (T_R) under this load is obtained from the expression:

$$q_R = \sigma \epsilon (T_R)^4$$

where ϵ , (surface coating emissivity) = 0.92

σ , (Stefan-Boltzmann constant) = 0.173×10^{-8}

T_R = average radiator surface temperature, R

Substituting these values into the above expression and solving for T_R , we get:

$$106.6 = (0.92) (0.173) \left(\frac{T_R}{100} \right)^4$$

$$T_R = 509^\circ\text{R} = 49^\circ\text{F}$$

The radiator coolant outlet temperature (T_2) is obtained from the expression:

$$q = (w) (C_p) (T_1 - T_2)$$



where q , (unit heat rejection rate) = 66.6 Btu/(hr)(sq ft)

C_p = average coolant specific heat

= 0.73 Btu/(lb)(F) for RS-89a (ethylene-glycol solution)
at 70 F

T_1 , (radiator coolant inlet temperature) = 80 F

T_2 = radiator coolant outlet temperature, F

w = unit area coolant flow rate

$$w = \frac{100 \text{ lb/hr}}{30 \text{ sq ft}} = 3.33 \text{ lb/(hr) (sq ft)}$$

Substituting these values into the above expression and solving for T_2 , we get:

$$q = 6.66 = (3.33) (0.73) (80 - T_2)$$

$$T_2 = 53 \text{ F}$$

The average radiator surface temperature (49 F) and the corresponding coolant outlet temperature (53 F) locate one point on the curve for $C_2 = 40 \text{ Btu/hr-ft}^2$ in Figure 22, which can be used in the construction of radiator performance maps as indicated below.

Let $C_2 = 40 \text{ Btu/(hr)(sq ft)}$ and let the radiator size be such that the equipment heat rejection rate is 60 Btu/(hr)(sq ft).

$$q_R = 60 + 40 = 100 \text{ Btu/(hr)(sq ft)}$$

Assuming $\epsilon = 0.8$,

$$q_R = 100 = (0.8) (0.173) \left(\frac{T_R}{100} \right)^4$$

$$T_R = 518 \text{ R} = 58 \text{ F}$$

From Figure 22, a corresponding coolant outlet temperature of 62°F is obtained on the $C_2 = 40$ curve. This temperature permits calculation of the radiator coolant inlet temperature based on the assumed flow rate of 3.33 lb/(hr)(sq ft).

$$q = 60 = (3.33) (0.73) (T_1 - 62)$$

$$T_1 = 86.7 \text{ F}$$

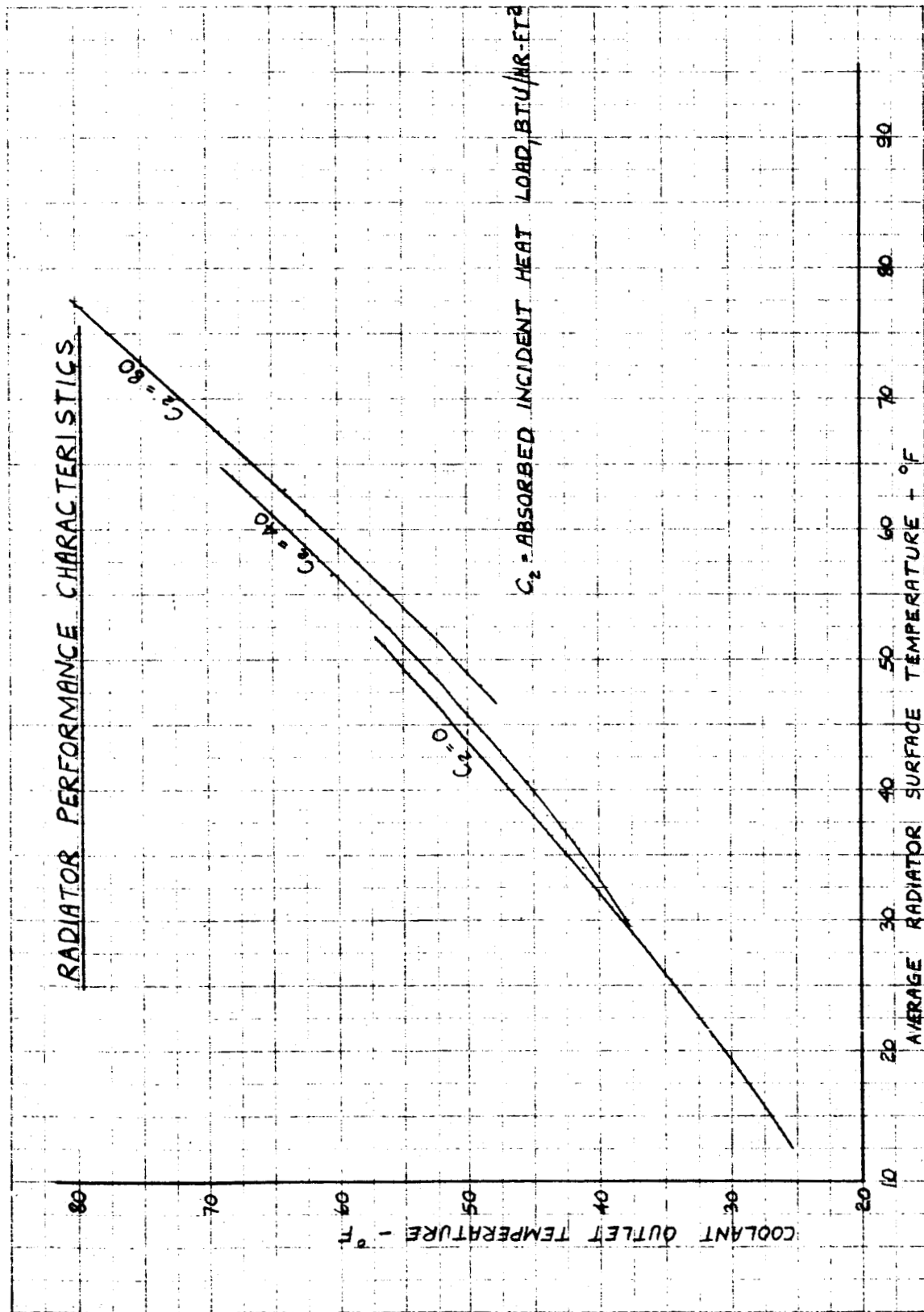


Figure 22. Radiator Surface Temperature Versus Coolant Outlet Temperature



This last temperature (86.7 F) and the corresponding equipment heat rejection rate, 60 Btu/(hr)(sq ft), locate one point on the curve for $\epsilon = 0.8$ in Figure 23, which also contains radiator performance data for emissivity values of 0.7 and 0.9. Similar curves have been established for the absorbed incident heat load range from 0 to 80 Btu/(hr)(sq ft), which is the variation expected under the environmental conditions of the mission profiles under consideration.

One problem inherent in the design of space radiators concerns the selection of a heat transport fluid which remains in the liquid state over the entire operating temperature range. Another desirable fluid property is a level of viscosity which does not increase drastically with a decrease in temperature. Large changes in viscosity tend to reduce fluid flow rates and enhance the possibility of the coolant freezing within the radiator and making it inoperative. To aid in the selection of candidate heat transport fluids, a family of curves has been calculated as exemplified by Figure 24. These curves indicate the variation in average radiator surface temperature with variation in heat load and surface emissivity. Temperatures were calculated with the expression:

$$q_E + C_2 = \epsilon \sigma T_R^4$$

where q_E = equipment heat load, Btu/hr per square foot of radiator area

C_2 = absorbed incident radiation, Btu/(hr)(sq ft)

ϵ = radiator surface emissivity

σ = Stefan-Boltzmann constant

T_R = average radiator surface temperature, R

Curves such as those shown in Figure 23 will be used for a preliminary determination of required radiator areas when equipment heat loads and operating temperature levels have been established. For a selected radiator surface emissivity and a radiator coolant inlet temperature based on the equipment operating temperature level, the equipment heat rejection rate per unit area is fixed by the curves of Figure 23, or similar ones for the appropriate absorbed incident heat load level at the design point. The effect of variation in absorbed incident heat load on radiator surface temperatures can then be obtained from curves such as those in Figure 24, which will indicate whether the selected combination of radiator surface emissivity and equipment heat rejection rate is compatible with coolant properties at low temperatures.

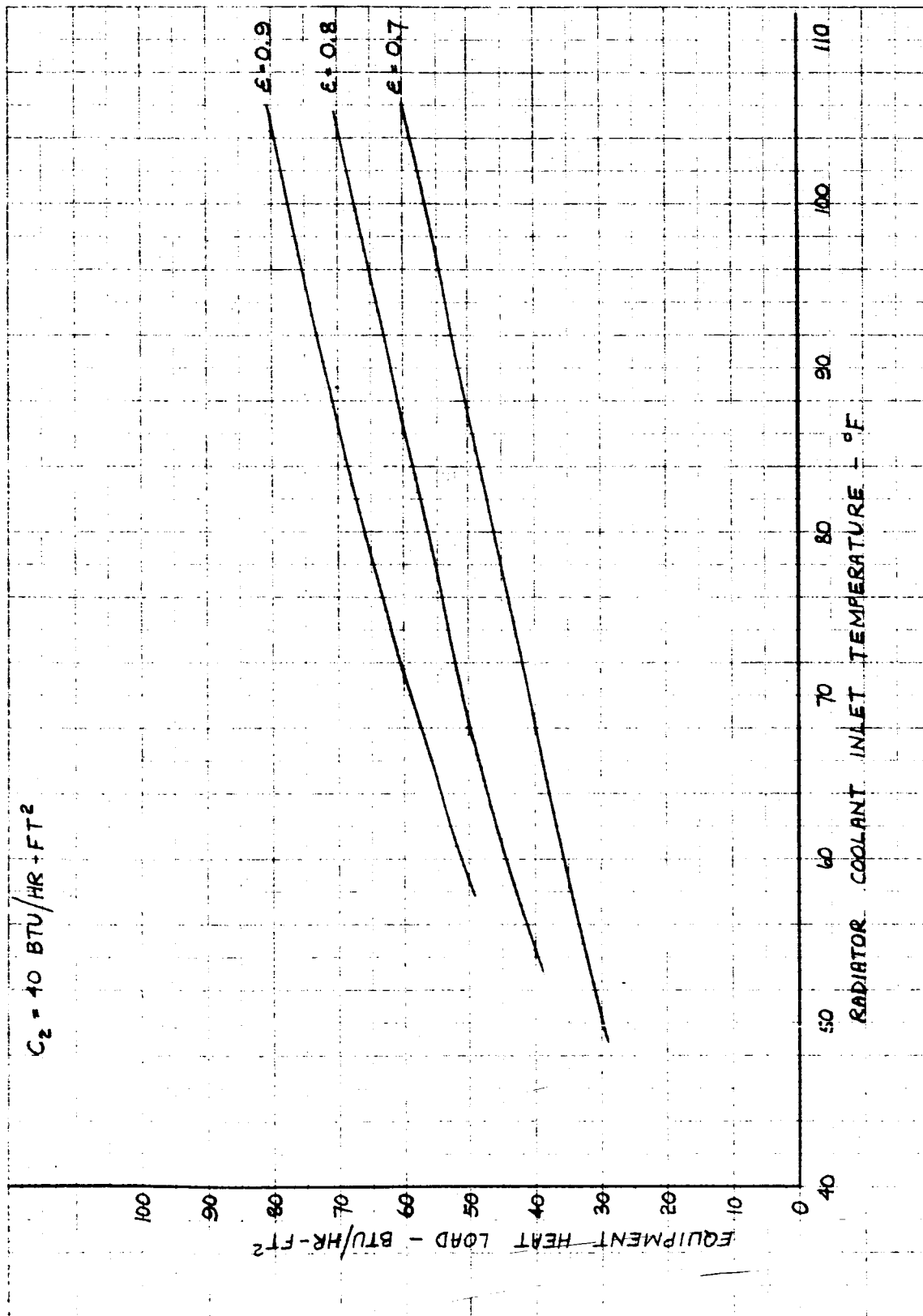


Figure 23. Coolant Inlet Temperature Versus
Equipment Heat Load

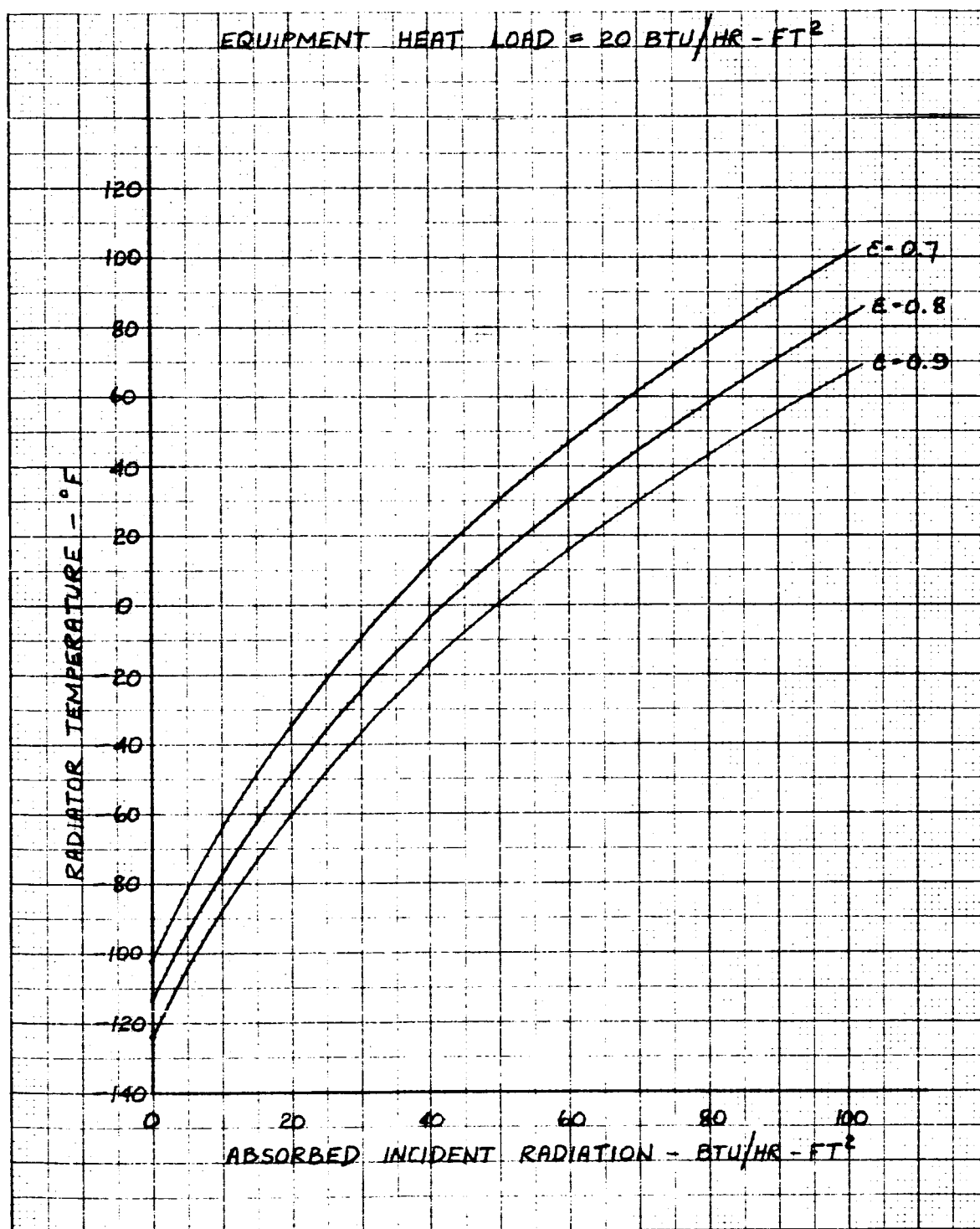


Figure 24. Radiator Temperature Versus Absorbed Incident Radiation



Another method of presenting the relationship between incident heat load and corresponding radiator performance is shown in Figure 25. In this illustration, the incident heat load is represented by the effective sink temperature; and the purpose of the curves is to show the minimum radiator heat load necessary to prevent freezing of the coolant. The method of obtaining the curves and their use are illustrated by the following example.

The maximum radiator heat load is established at the design point and may be represented by the expression:

$$q_{\max} = \epsilon \sigma (T_4)^4$$

where $q_{\max} = q_E + C_2$

q_E = equipment heat load, Btu/(hr)(sq ft)

C_2 = absorbed incident radiation, Btu/(hr)(sq ft)

σ = Stefan-Boltzmann constant = 0.173×10^{-8} Btu/(hr)(sq ft)(°R)⁴

ϵ = radiator surface emissivity

T_R = average radiator surface temperature, R

The minimum radiator heat load required to prevent freezing is obtained from the expression

$$q_{\min} = \epsilon \sigma (T_f^4 - T_s^4)$$

where T_f = coolant freezing temperature, R

T_s = effective sink temperature, R

$$\frac{q_{\min}}{q_{\max}} = \frac{T_f^4 - T_s^4}{T_R^4}$$



For the condition represented by Figure 25, $q_E = 50 \text{ Btu}/(\text{hr})(\text{sq ft})$, $C_2 = 80 \text{ Btu}/(\text{hr})(\text{sq ft})$, and $\epsilon = 0.9$. The corresponding radiator coolant inlet temperature is obtained from a curve similar to Figure 23 and is 101 F.

$$\Delta T_c, \text{ coolant radiator temperature drop, } = \frac{q_E}{w C_p}$$

$$= \frac{50 \text{ Btu}/(\text{hr})(\text{sq ft})}{(0.73 \text{ Btu}/\text{lb-}^\circ\text{F})(3.33 \text{ lb}/\text{hr-ft}^2)} = 20.6 \text{ F}$$

$$T_2 = \text{coolant radiator outlet temperature}$$

$$= 101 - 20.6 = 80.4 \text{ F}$$

From Figure 22, $T_R \approx 79 \text{ F} = 539 \text{ F}$ at $C_2 = 80 \text{ Btu}/(\text{hr})(\text{sq ft})$

$$\left(\frac{T_R}{100}\right)^4 = \left(\frac{539}{100}\right)^4 = 844$$

Assuming $T_f = 400 \text{ R}$ and $T_s = 300 \text{ R}$,

$$\frac{q_{\min}}{q_{\max}} = \frac{\left(\frac{400}{100}\right)^4 - \left(\frac{300}{100}\right)^4}{844} = 0.207$$

This ratio and the assumed sink temperature of 300 R locate one point on the curve for $T_f = 400 \text{ R}$ in Figure 25. Other curves are shown for coolant freezing temperatures of 420 R, 440 R, and 460 R, respectively. These curves define the minimum radiator heat loads necessary to prevent freezing of the coolant as a function of the effective sink temperature based on $q_{\max} = q_E + C_2 = 130 \text{ Btu}/(\text{hr})(\text{sq ft})$. The dashed q_{\min} line in Figure 25 represents the equipment heat load of $50 \text{ Btu}/(\text{hr})(\text{sq ft})$ which is located by the ratio $50/130 = 0.385$. The significance of this line is that freezing will not occur under any sink temperature condition if the coolant freezing point is below approximately 424 R. However, if the freezing point of the selected coolant is 460 R and the effective sink temperature is 0°R , the amount of heat which must be added to the coolant loop to prevent freezing is indicated by the difference between the dashed line and the curve representing $T_f = 460^\circ\text{R}$. This quantity is calculated to be

$$(0.530 - 0.385)(130) = 18.85 \text{ Btu}/(\text{hr})(\text{sq ft})$$

Likewise, Figure 25 indicates that heat addition to prevent coolant freezing will not be necessary for any of the four freezing

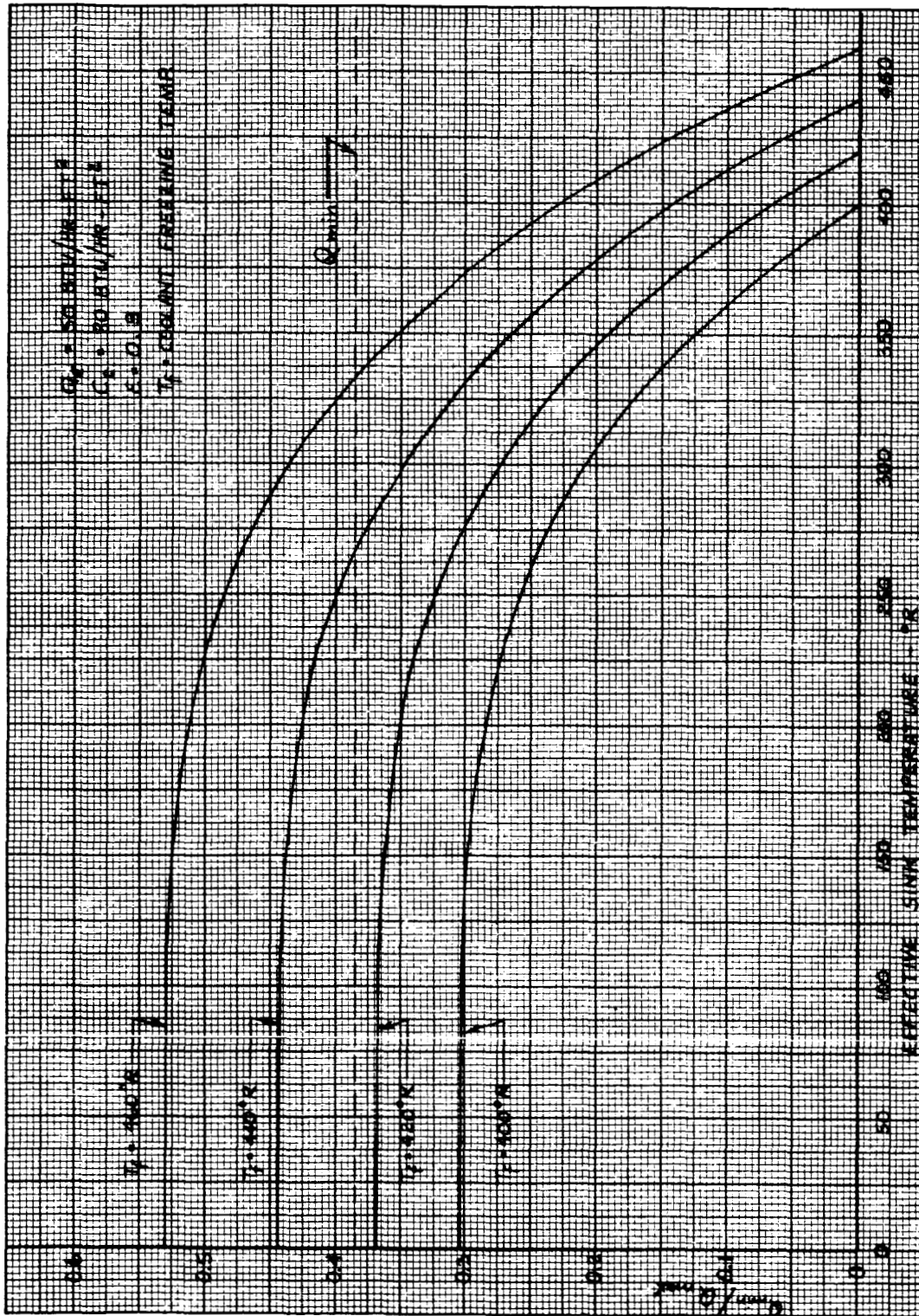


Figure 25. Q_{\min}/Q_{\max} Ratio Versus Sink Temperature



temperatures shown if the sink temperature remains above approximately 333°R. Obviously, Figure 25 is applicable only to one radiator design condition; and other curves have been constructed to cover the probable range of equipment and incident heat loads at the design point.

2.3.3 Coolant Viscosity

For every space radiator configuration which may be considered in the course of this study, it is expected that the coolant flow rate will be such that laminar flow conditions will exist within the radiator. Under this condition, the system pressure drop will be proportional to the product of flow rate and viscosity, or

$$\Delta p \propto \dot{w} \mu$$

If it is assumed that a temperature control system will regulate coolant temperatures within a control band, then the coolant flow rate and pressure drop will remain constant except in that portion of the system where the temperature and, hence the viscosity are permitted to vary. This temperature variation occurs in the space radiator when the incident heat load changes due to variation in orbital position and spacecraft orientation. Therefore, if the radiator pressure drop is to remain constant when the coolant viscosity increases, the flow rate must decrease accordingly. This relationship is illustrated in Figure 26, which is based on the above proportionality. For example, if the flow rate is reduced to 40 per cent of the design value, the viscosity may increase by a factor of 2.5 without causing an increase in pressure drop.

Another type of plot which is expected to aid in the selection of a suitable coolant is illustrated in Figure 27. This plot shows the relationship between radiator outlet temperature and maximum allowable coolant viscosity for a number of equipment heat rejection rates. The allowable viscosity is based on a design coolant flow rate of 3.33 lb/(hr)(sq ft) of radiator surface area, a design coolant viscosity of 5.0 lb/(hr)(ft), and a constant coolant specific heat of 0.80 Btu/(lb)(F). Radiator coolant inlet temperature is assumed to be constant at 80°F, and the equipment heat loads are shown on the basis of required heat rejection per square foot of radiator area. Radiator outlet temperatures were calculated with the equation

$$q_E = (\dot{w}) (C_p)(80 - T_2)$$

where q_E = equipment heat load, Btu/(hr)(sq ft)

C_p = coolant specific heat, Btu/(lb)(F)

T_2 = radiator outlet temperature, °F

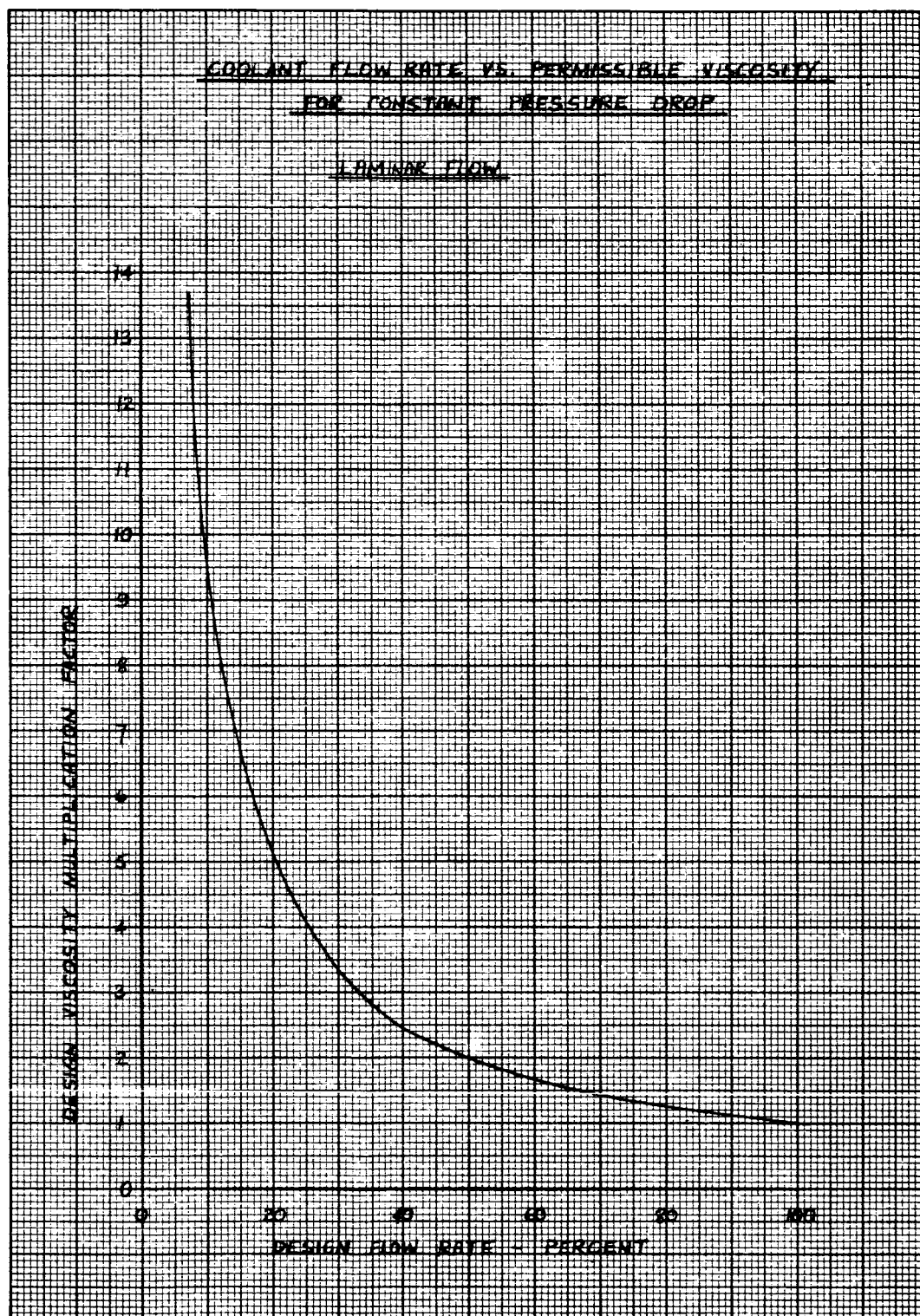


Figure 26. Viscosity Multiplication Factor
Versus Flow Rate

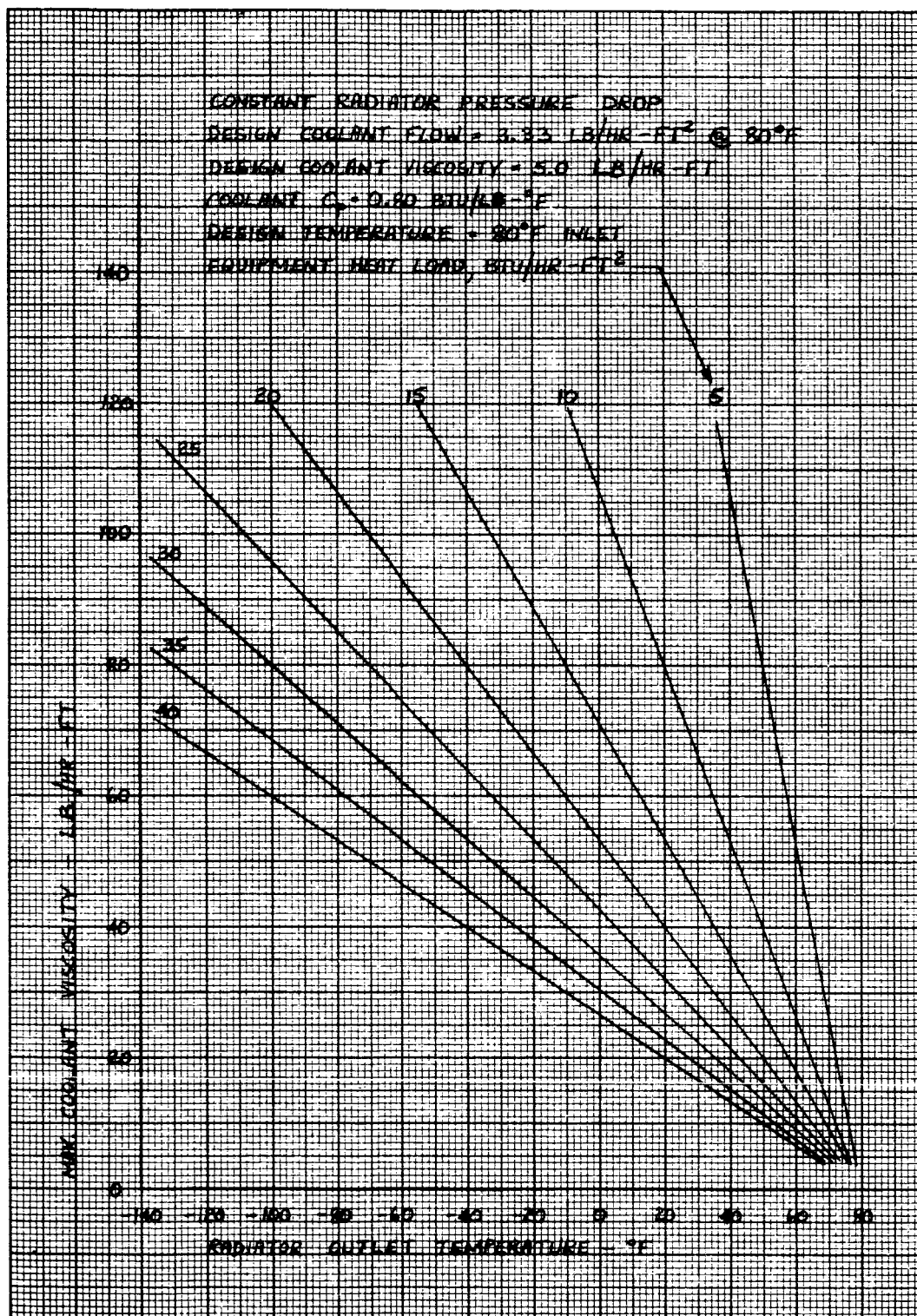


Figure 27. Viscosity Versus Radiator Outlet Temperature



The value of coolant viscosity corresponding to each selected flow rate was determined by maintaining a constant value for the product of flow rate and viscosity, calculated at the design point. For the example illustrated in Figure 27, this product is $16.65 \text{ (lb)}^2 / \text{(hr)}^2 \text{(ft)}^3$. Assuming a flow rate of $2.0 \text{ lb/(hr)(sq ft)}$, the allowable viscosity to maintain a constant pressure drop is

$$\frac{16.65}{2.0} = 8.33 \text{ lb/(hr)(ft)}$$

For an equipment heat load of $40 \text{ Btu/(hr)(sq ft)}$,

$$40 = (2.0)(0.80)(80 - T_2)$$

$$T_2 = 55^\circ\text{F}$$

This temperature and the viscosity value of 8.33 lb/(hr)(ft) locate one point on the $40 \text{ Btu/(hr)(sq ft)}$ line in Figure 27. Other equipment heat loads are shown to illustrate the allowable viscosity range for one set of design conditions. Similar curves have been established to cover a range of design viscosity values and specific heats.

Another method of presenting coolant viscosity design data is illustrated in Figure 28, which represents a cross-plot of data in Figure 27. In this method, allowable coolant viscosity is shown as a function of equipment heat load, with radiator outlet temperature as a parameter. This type of plot demonstrates clearly the large variation in allowable coolant viscosity with change in equipment heat load at constant radiator outlet temperature.

2.3.4 α/ϵ Ratio Selection

The simplest approach to control freezing may be by controlling the α/ϵ ratio of the radiator surface. The greatest value for emissivity (ϵ) at radiator temperature with a given α/ϵ ratio gives the greatest radiator efficiency and this is shown in Figure 29. The continuous nature of the curves was obtained by postulating combining two surfaces in any ratio. The solar absorptivity (α) appears only in subsequent equations as part of the α/ϵ ratio. The derivation of the equation of the factors which determines the minimum required α/ϵ ratio is shown below.

For a flat plate at an angle θ from the sun's rays,

$$\text{heat received from the sun, } Q_S = 442 \alpha A \cos \theta \left(\frac{1}{AU} \right)^2$$

$$\text{and heat emitted to space, } Q_E = \sigma \epsilon A (T_s^4 - T_{space}^4) \quad T_{space} \cong 0$$

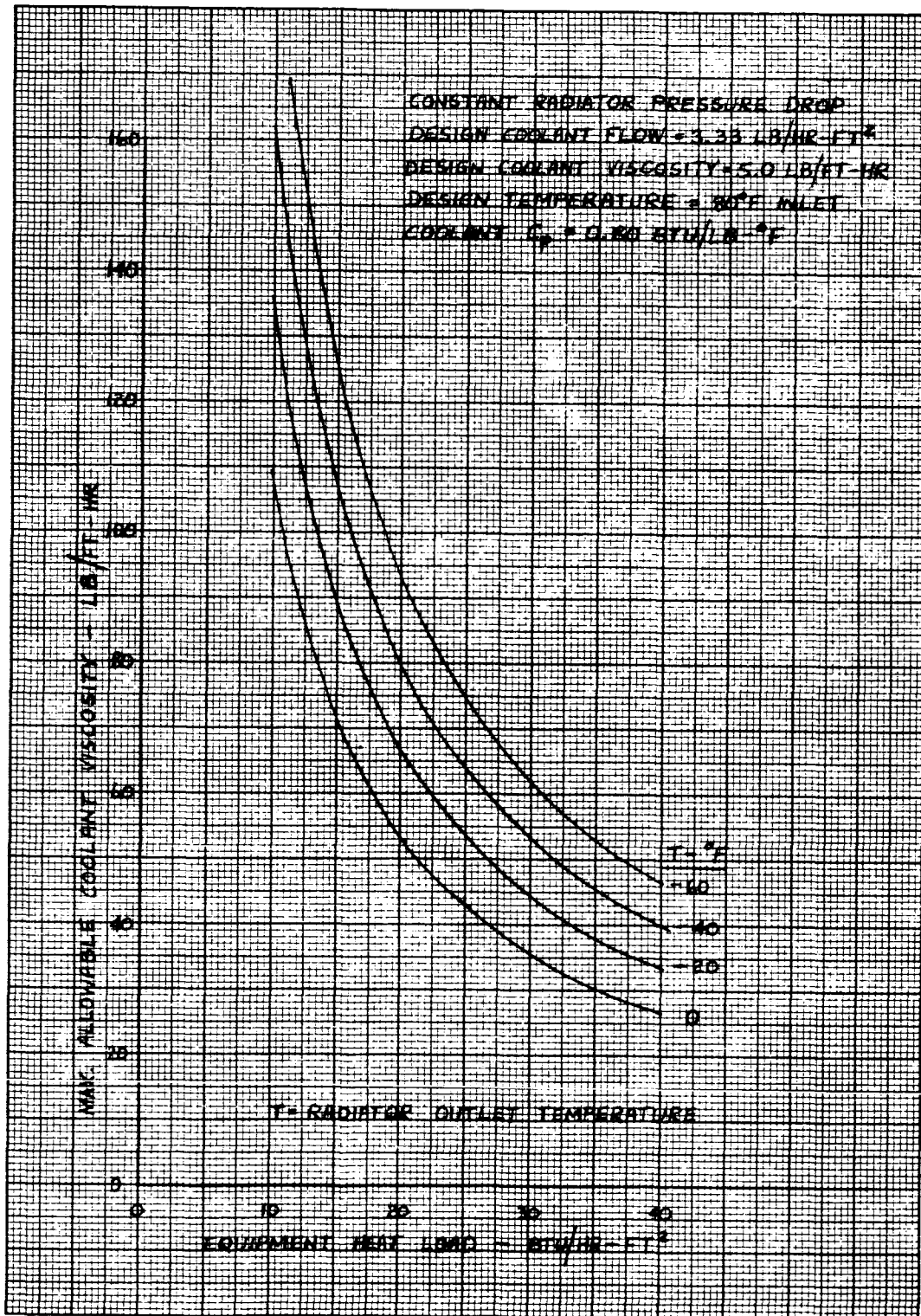


Figure 28. Viscosity Versus Equipment Heat Load

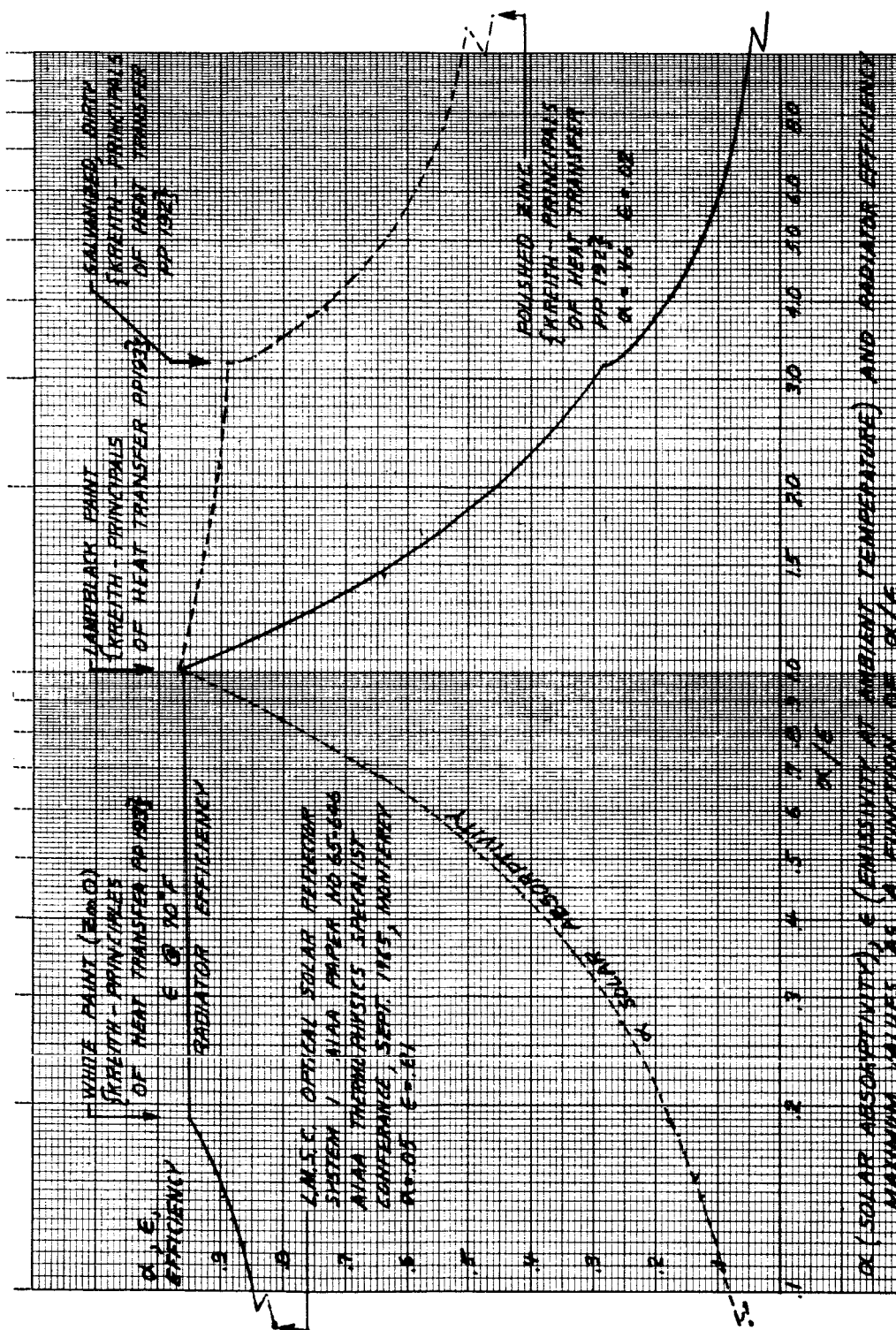


Figure 29. Radiator Efficiency Versus α/ϵ Ratio



For a condition of equilibrium where heat input exactly balances heat output to exist, Q_S must equal Q_E :

$$442 \alpha A \cos \theta \frac{1}{(AU)^2} = \sigma \epsilon A T_S^4$$

The equilibrium temperature (T_S) can be solved as:

$$T_S = \sqrt[4]{\frac{442 \alpha \cos \theta}{\sigma \epsilon (AU)^2}} \quad (1)$$

$$\text{or } T_S^4 = \frac{442 \alpha \cos \theta}{\sigma \epsilon (AU)^2}$$

The equilibrium temperature as a function of α/ϵ is shown in Figure 30. This graphically presents the equilibrium temperature as a function of α/ϵ ratio, distance from the sun (AU) and surface orientation or configuration. By selecting equilibrium temperatures corresponding to the freezing (or viscosity limiting) temperatures with the appropriate AU and surface orientation the approximate radiator α/ϵ ratio can be obtained. Figure 29, which shows ϵ and radiator efficiency as a function of α/ϵ ratio can then be examined to see if the α/ϵ ratio gives a reasonably high radiator efficiency and what it would be.

When heat from any or all possible sources (Q_D) is added, the total energy radiated to space is $Q_E' = Q_S + Q_D$ or

$$Q_D = Q_E' - Q_S = \sigma \epsilon A (T_S')^4 - \sigma \epsilon A (T_S)^4 = \sigma \epsilon A (T_S'^4 - T_S^4) \quad (2)$$

where T_S' is the radiating temperature. This is identical to rejecting heat to the equilibrium temperature (T_S) by radiation.

The equilibrium temperature serves as the sink temperature to which the radiator rejects energy. A first approximation of radiator size can be made using this sink temperature and radiator efficiency (assuming the radiator temperature at fluid out temperature).

When no heat is transferred ($Q_D = 0$) the radiator can fall to equilibrium temperature ($T_S' = T_S$). If this temperature is above the freezing or viscosity limiting point of the radiator fluid, no problem can take place. If there is a minimum heat rejection (Q_D), the temperature which will reject it can be calculated from Equation (2). All that is required is that at no point should this temperature drop below the freezing or viscosity limiting point of the radiator fluid (T_S'). Using Equation (2), and solving for α/ϵ , we get:

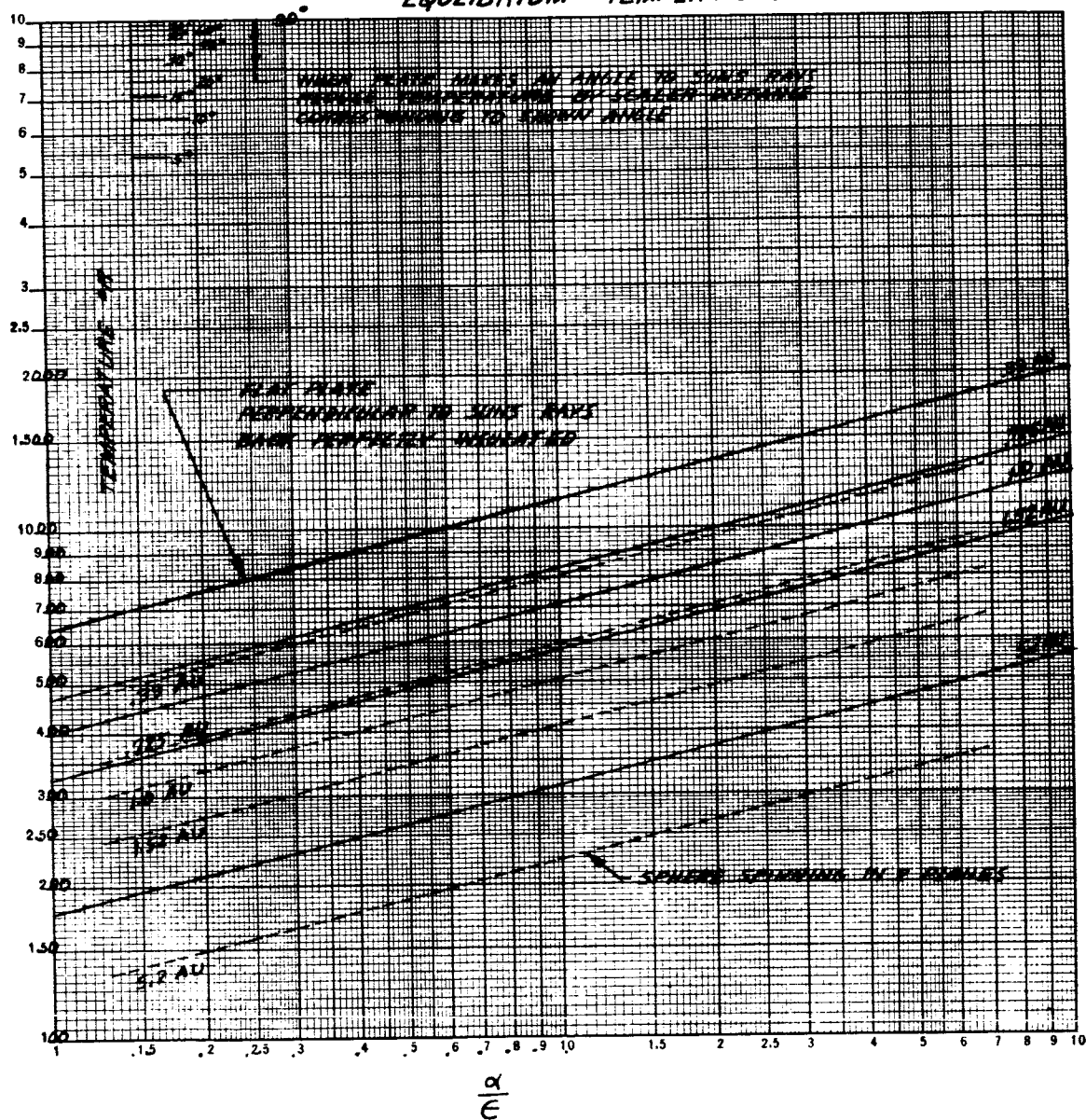


Figure 30. Equilibrium Temperature Versus α/ϵ Ratio



$$\begin{aligned}\frac{Q_D}{\sigma \epsilon A} &= (T_s')^4 - (T_s)^4 \\ (T_s)^4 &= -\frac{Q_D}{\sigma \epsilon A} + (T_s')^4 = \left(\frac{\alpha}{\epsilon}\right) \left(\frac{442}{\sigma}\right) \frac{\cos \theta}{(AU)^2} \\ \frac{\alpha}{\epsilon} &= \frac{\sigma (AU)^2}{442 \cos \theta} \left[(T_s')^4 - \frac{Q_D}{\sigma \epsilon A} \right] \quad (3)\end{aligned}$$

If T_s' is the fluid minimum temperature (freezing or viscosity limiting point) and Q_D is the lowest value, Equation (3) can be used to calculate minimum required α/ϵ ratio.

Space and Information Systems Division of North American Aviation has developed a computer program which can give the energy input due to reflected solar (Q_{SR}) and planet emission (Q_{EE}) (as well as direct solar input) as a function of orbit and position. This information can be considered as part of Q_D/A in Equation (3).

It can be shown however that the heat received from solar reflection

$$Q_{SR} = \frac{442 A \bar{A}_L}{(AU)^2} \left(1 - \sqrt{1 - \frac{r^2}{(r+h)^2}} \right) \cos \psi$$

and $\cos \psi$ and subsequent $\cos \beta$ are complicated functions of orbital position and surface orientation. Likewise, it can be shown that the heat received from earth (or planet) emission

$$Q_{EE} = (1 - \bar{A}_L) \sigma A \left(1 - \sqrt{1 - \frac{r^2}{(r+h)^2}} \right) \cos \beta \left[(T_p)^4 - (T_s')^4 \right]$$

If, however, the total heat load is at a minimum for a short period of time only, the heat capacitance of the radiators, if they are initially above the freeze temperature, can be counted on to help during the period of minimum heat rejection. This can be determined from the equation:

$$Q = \frac{M C_p \Delta T}{\Delta t} = \frac{(M C_p)_R (T_i - T_s')}{\Delta t} \quad \text{where } \Delta t = \text{time in hours}$$

The resulting equation may then be rewritten as follows for a flat plate at angle θ to sun's rays.



$$\frac{\alpha}{\epsilon} = \frac{(AU)^2}{442 \cos \theta} \left\{ \sigma (T'_S)^4 - \frac{Q'_D}{\epsilon A} - \frac{M_R C_{P_R} (T_i - T'_S)}{\epsilon A \Delta t} - \frac{442 \bar{A}_L}{\epsilon (AU)^2} \left(1 - \sqrt{1 - \frac{r^2}{(r+h)^2}} \right) \cos \psi \right. \\ \left. - \frac{(1 - \bar{A}_L) \sigma}{\epsilon} \left(1 - \sqrt{1 - \frac{r^2}{(r+h)^2}} \right) \cos \beta \left[(T_A)^4 - (T'_S)^4 \right] \right\} \quad (4)$$

A	= surface area
(AU)	= astronomical unit (distance from the earth to the sun, 92,900,000 miles)
\bar{A}_L	= planet albedo
h	= orbit height from planet surface, miles
$M_R C_{P_R}$	= radiator capacitance
Q'_D	= heat input from sources such as circulating coolant
T_P	= effective planetary surface temperature
T'_S	= freezing or viscosity limiting temperature of radiator at any point (time)
Δt	= time period when the radiator capacitance heat flows outward
β	= equivalent incidence angle (earth emission absorption)
ϵ	= surface emissivity
θ	= angle between radiating surface and solar rays
σ	= Stefan-Boltzmann constant, $.1714 \times 10^{-8}$
ψ	= equivalent incidence angle (solar reflective)

This Equation (4) may be solved point by point by a computer or manually by selection of those times which appear most critical to give the α/ϵ required to prevent freezing. Initially trials of course will select T'_S at the freezing temperature of water (the most efficient heat transfer fluid) and if the α/ϵ ratio is 1 or less for a given mission, water may be used. If α/ϵ is very high then the freezing temperature of a water glycol solution may be tried. If α/ϵ is still much greater than 1, then the problem of preventing freezing will require investigation of other possible fluids and other techniques to control the temperature.

If the radiator surface does not see the sun, the terms inside the bracket must be equal to zero.



$$\begin{aligned} \therefore (T_S')^4 + \frac{M_R C_{PR}}{\sigma \epsilon A \Delta t} (T_S') &= \frac{Q_D'}{\sigma \epsilon A} + \frac{M_R C_{PR} T_i}{\sigma \epsilon A \Delta t} + \frac{4.42 \bar{A}_L}{\epsilon (AU)^2} \left(1 - \sqrt{1 - \frac{r^2}{(r+h)^2}} \right) \cos \psi \\ &+ \frac{1 - \bar{A}_L}{\epsilon} \left(1 - \sqrt{1 - \frac{r^2}{(r+h)^2}} \right) \cos \beta \left[(T_P)^4 - (T_S)^4 \right] \end{aligned}$$

This is another way of stating that at the coolest point on the radiator, the permissible freezing temperature will be such that it rejects heat from the radiator segment equal to the total heat input to that radiation segment. T_S' is the temperature which determines whether water, water glycol or some other fluid will be necessary to prevent radiator freeze up, or possible that some other approach to the freezing problem be taken.

Once the minimum α/ϵ ratio and fluid have been determined or some other solution to freezing utilized, the freezing condition for the radiator will have been taken care of. It is then possible to design the radiator around conditions of maximum heat input Q_S only in a conventional manner.



3.0 FORECAST FOR NEXT QUARTER

The three major tasks initiated during the previous quarter will be completed during the next quarter.

The thermal requirements of the astrionic equipment will be established. This will involve completing the survey of the development trend in astrionic equipment, in the packaging of the equipment, and the establishment of the heat loads, operating temperatures and temperature regulation requirements. The various astrionic equipment required for the various missions selected for the study will be determined. The heat load profiles developed in this manner will be considered to be representative of those to be expected for future Saturn missions. These equipment heat load profiles plus the incident heat loads for the various missions will define the heat rejection requirements. The maximum and minimum heat load conditions for the selected missions will be established by considering the various vehicle attitude in flight, the surface orientation with respect to the heat sources, the vehicle spin rate and the spin axis. With the completion of this effort, all the necessary basic requirements and constraints will have been established.

The survey of current and new development in astrionic equipment and thermal control components and processes will be expanded to include as much of the total industry as possible. Survey data will be compiled in convenient forms. The survey results will be reviewed and evaluated to establish the feasible methods or processes, components and subsystems. Also, the development status and area requiring further research or investigation will be reviewed and recommendations will be made.

Various concepts for the astrionic equipment ECS and overall thermal control systems will be synthesized for evaluation and preliminary selections will be made for detailed analysis. The analytical data will be presented in parametric form for convenience in evaluating and comparing the various concepts. The primary parameters will be mission duration (or operational duration), temperature, and heat loads. In addition, for the convenience of data presentations, many other parameters will be used. In performing the analytical study, any assumptions that are made will be indicated and justifications given.